6-1-1971

The Instantaneous Unit Hydrograph: Its Calculation By The Transform Method And Noise Control By Digital Filtering

A. R. Rao

J. W. Delleur
delleur@purdue.edu

TECHNICAL REPORT NO. 20

THE INSTANTANEOUS UNIT HYDROGRAPH:

ITS CALCULATION BY THE TRANSFORM METHOD AND NOISE CONTROL BY DIGITAL FILTERING

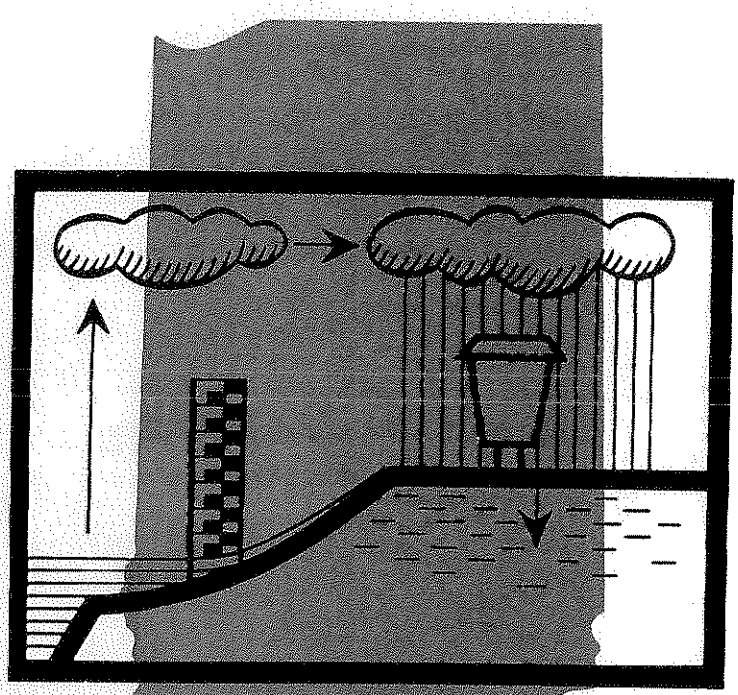

by

Ramachandra A. Rao

J. W. Delleur

June 1971

PURDUE UNIVERSITY
WATER RESOURCES RESEARCH CENTER
LAFAYETTE, INDIANA

School of Civil Engineering

Purdue University

Lafayette, Indiana 47907

THE INSTANTANEOUS UNIT HYDROGRAPH:

ITS CALCULATION BY THE TRANSFORM METHOD AND NOISE CONTROL BY DIGITAL FILTERING

by

Ramachandra A. Rao

J. W. Delleur

Period of Investigation: June 1970 - July 1971

Partial Report for OWRR B-008 and B-022-IND

Matching Grant Agreement Numbers 14-01-0001-1902 and 14-01-0001-3080

Purdue University Water Resources Research Center

Technical Report No. 20

June 1971

PREFACE AND ACKNOWLEDGMENTS

This report presents an extension of the work on linear system analysis in surface hydrology supported by the Office of Water Resources Research, Department of the Interior under project OWRR A-001-IND entitled "Estimation on Runoff from Small Watersheds in Indiana".

The work presented herein was supported partly by the Office of Water Resources Research under projects OWRR B-008-IND (Assembly and Analysis of Hydrologic and Geomorphologic Data for Small Watersheds in Indiana) and OWRR B-022-IND (Effects of Urbanization in Hydrology) and partly by the Purdue Research Foundation under grants XR 5869 and XR 5997. J. W. Delleur is the director for the above mentioned projects and A. R. Rao is the principal investigator for project B-022-IND.

The material of sections 2.1 and 2.2 related to the Fourier and Laplace transforms has been condensed from the Doctoral Thesis of Mr. D. Blank, under the direction of J. W. Delleur. The computational and numerical aspects which were not dealt with in depth before have been analyzed in detail and are reported in sections 2.4 and 2.5. The initial trials on noise filtering were done by D. Blank and J. W. Delleur and are reported in reference 10. The authors wish to express their appreciation to Dr. D. Blank and Dr. P. B. S. Sarma who compiled the data on rural and urban watersheds, respectively, used in this report, to Mr. J. Parker who developed the computer programs for the Laplace transform, and to Mr. M. T. Lee who wrote the computer programs for the Z-transform and for the filtering in the frequency domain.

ABSTRACT

The report covers an extension of the work performed under project number OWRR A-001-IND entitled "Estimation of Runoff from Small Watersheds in Indiana". The results of the previous work were summarized by D. Blank and J. W. Delleur in Purdue University Water Resources Research Center Technical Report No. 4 of August 1968 entitled "A Program for Estimating Runoff from Indiana Watersheds - Part I Linear System Analysis in Surface Hydrology and its Application to Indiana Watersheds". This initial work consisted of two parts: 1. the acquisition of a library of rainfall excess and direct runoff data, and 2. the extension of linear system analysis methodologies using principally the Fourier transform for predicting the surface runoff from observed rainfall. A summary of the second part is scheduled for publication in Water Resources Research (see ref. 10).

The extension of this work including the use of the Laplace and Z-transforms, their limitations and the effect and characterization of noise in the data have been presented in a summary form by Delleur and Rao (see refs. 17 and 18). The present report brings the several results related to the estimation of the instantaneous unit hydrograph under a single cover.

The rainfall excess - direct runoff relationship on a watershed was assumed to be expressible by the convolution integral

$$y(t) = \int_0^t h(\tau)\, x(t-\tau)\, d\tau$$

where $y(t)$ is the output function (direct runoff hydrograph)

$x(t)$ is the input function (excess precipitation), and

$h(t)$ is the kernel function (impulsive response).

Linear system analysis techniques were used to evaluate the kernel function (instantaneous unit hydrograph). The methods used were the Fourier, the

Laplace and the Z-transforms. The Z-transform requires the least computer time, but the Fourier transform provides the best insight in the understanding of the methodology. Oscillations of the kernel functions are often observed. These may be generated by the computational procedure or may be due to noise in the data. The oscillations due to the computational procedure are, in general, related to the discretization rate, and they can often be controlled by increasing the time step in the discretization of the data. The oscillations due to noise in the data usually can be controlled by digital filtering. A combination of careful selection of the digitization rate and of digital filtering of the data gives best results. Alternatively the kernel function in the time domain or the transfer function in the frequency domain may be smoothed. The numerical calculation techniques are discussed. Of particular importance are the selection of the truncation values in the numerical integrations in the transform domain, the selection of the proper number of intervals in these integrations and in the discrete convolution which approximates the convolution integral.

The properties of the noise attributable to the rainfall excess data are discussed; the noise spectrum and its probability distribution are estimated.

Finally the computational techniques are illustrated by means of a theoretical example and several examples making use of data from rural and urban watersheds located in Indiana.

The results obtained in this investigation will be used in research currently in progress in the areas of rural and urban hydrology at the Purdue University Water Resources Research Center.

TABLE OF CONTENTS

TABLE OF CONTENTS

(continued)

LIST OF SYMBOLS

f	frequency, cycles per unit of time
$f(t)$	function of time
f_c	Nyquist frequency
$f^*(t)$	discrete sampled function of $f(t)$
$f^*(s)$	Laplace transform of $f^*(t)$
$f(\omega)$	Fourier Transform of $f(t)$
$g(t)$	function defined in Eq. 17
$G(q)$	function defined in Eq. 16
$h(t)$	impulsive response
H_n	coefficient defined in Eq. 39
$H(n\Delta t)$	pulsed impulsive response, i.e. inverse of $H(z)$
$H(s)$	Laplace transform of $h(t)$
$H(z)$	Z-transform of $h(n\Delta t)$
$H(\omega)$	Fourier transform of $h(t)$
i	counter index in Eqs. 54 through 64
j	imaginary quantity, $\sqrt{-1}$
n	counter index in Eqs. 32 through 40
N	number of sampling points in discrete Fourier transform, Eqs. 43, 44
N_P	number of sampling points in rainfall excess hyetograph
N_Q	number of sampling points in direct runoff hydrograph
N_ω	number of sampling points in frequency response $H(\omega)$
q	real part of Laplace transform variable s
q_m	maximum value of q used in numerical calculation
$R_e(s)$	real axis in transform domain
$R_g(q)$	real part of $G(q)$
$R_h(\omega)$	real part of $H(\omega)$
$R_x(\omega)$	real part of $X(\omega)$

LIST OF SYMBOLS
(continued)

$R_y(\omega)$	real part of $Y(\omega)$
s	Laplace variable = $\gamma + jq$
t	time
T_c	period corresponding to the frequency interval Δf
T_K	base time of kernel function
T_Q	base time of direct runoff hydrograph
T_R	rainfall excess duration
$w(t)$	impulsive response of filter
w_i	coefficient in discrete filter, Eqs. 54, 60
w_o	coefficient in discrete filter, Eqs. 56, 61, 62
$W(\omega)$	frequency response of filter
$x(t)$	input function, i.e. rainfall excess
$x(n\Delta t)$	sampled input function
$X(q)$	Laplace transform of $x(t)$
$X(z)$	Z-transform of $x(n\Delta t)$
$X(\omega)$	Fourier transform of $x(t)$
$X_h(\omega)$	imaginary part of $H(\omega)$
$X_g(q)$	imaginary part of $G(q)$
$X_x(\omega)$	imaginary part of $X(\omega)$
$X_y(\omega)$	imaginary part of $Y(\omega)$
$y(t)$	output function, i.e. direct runoff
$y(n\Delta t)$	sampled output function
$Y(q)$	Laplace transform of $y(t)$
$Y(z)$	Z-transform of $y(n\Delta t)$
$Y(\omega)$	Fourier transform of $y(t)$
z	Z-transform variable

LIST OF SYMBOLS
(continued)

γ	real part of s
δ	Dirac δ function
$\theta(\omega)$	phase of filter
τ	time
ω	angular frequency
ω_c	Nyquist frequency
Ω	$2\pi/N\Delta t$

For the list of notations used in figures, see lower part of page 16

LIST OF FIGURES

I. INTRODUCTION

In formulating a model of the response of a watershed we conceptualize the physical processes and express them in mathematical terms. These conceptualizations may be deterministic or stochastic, linear or nonlinear, lumped or distributed, time independent or time varying, stationary or nonstationary or some combination of these. The choice of the model is determined by the type of problem to be solved. For example, stochastic models have been used successfully for the simulation of monthly flows. The St. Venant's equations provide a nonlinear deterministic model of the flood wave propagation which has been used successfully in modeling floods in large streams as the Ohio River, and its simplified version known as the kinematic wave theory has been successfully and particularly used in modeling the overland flow process. As may be seen from these examples, the time scale of the problem and the signal to noise ratio govern to a great extent the choice of the model.

This report addresses itself to the modeling of transient phenomena due to a single storm on a relatively small rural watershed, smaller than 500 square miles, for example. This problem is effectively treated by a deterministic model as the storm and runoff signals are usually large compared to the noise or error that they may contain. Among the several deterministic models possible the lumped linear system is the simplest. It has the advantage of being a generalization of the unit hydrograph, a familiar tool to hydrologists. The lumping of the input may appear to be an oversimplification. However, the average number of raingages in Indiana, for example, is one per 250 square miles, and there is no simple alternative to that of lumping the rainfall excess input. The assumption of linearity may also appear as an oversimplification. However, the impulsive response calculated by the linear system theory is the leading term of a sequence of responses

of pure first, second, third, etc. order systems. The sum of r of these responses is the output of a nonlinear polynomial system of order r. As a result, in the majority of the cases the linear system approach yields a method of estimation of runoff with a degree of accuracy that is sufficient for many engineering design purposes. The assumption of linearity may be limited to the storm under analysis by allowing the parameters of an otherwise linear model to vary from storm to storm as a function of the input. Sarma, et al.[7] have used this type of "quasilinear" system to model the rainfall-runoff process in urbanized watersheds.

A number of deterministic models in hydrology consider the rainfall and runoff as cause and effect. In surface water hydrology it is customary to separate the ground water component from the surface runoff; the cause and effect relationship is then between the runoff producing rainfall or effective rainfall and the direct runoff. In 1932 Sherman[1] postulated that there is a linear relationship between effective rainfall (cause) and direct runoff (effect). He defined the unit hydrograph as the response of the watershed to a specified effective rainfall input, namely a unit depth of effective rainfall applied uniformly over the catchment in a specified time duration. The limit of the unit hydrograph as the rainfall duration approaches zero is called the instantaneous unit hydrograph (IUH). J. C. I. Dooge[2] developed the basic theory of the instantaneous unit hydrograph. The IUH can be thought of as the impulse response of a lumped, time invariant linear system. For this type of system the mathematical relationship between the input and output function is the convolution or Duhamel integral

$$y(t) = \int_0^t x(\tau)h(t - \tau)d\tau \qquad (1)$$

where $x(t)$ and $y(t)$ are the input and output functions, respectively, and $h(t)$ is the impulse response or the kernel function.

An effective method of analysis of lumped linear hydrologic systems is the transform approach. Levi and Valdes[3] and Diskin[4] suggested the use of the Fourier and of the Laplace transforms, respectively, but did not perform the necessary numerical inversions. Yamaoka and Fujita[5] bypassed the inversion of the Fourier transform by using the technique of the Nyquist plots. Blank and Delleur[6] applied the Fourier transform and its inversion to the kernel (instantaneous unit hydrograph) identification of more than 1000 storms over more than 50 watersheds in Indiana with areas varying from 3 to 300 square miles. Sarma, Delleur, and Rao[7] used this method to identify the kernel functions of urban watersheds. They found that for small urban basins, perhaps less than 5 square miles, the kernel functions obtained by the transform method may be closely approximated by the kernel function corresponding to a single linear reservoir.

The estimation of impulse response functions has received considerable attention[8]. Once the impulse response function describing the effective rainfall-direct runoff transfer is identified, it can be used for estimating the direct runoff resulting from an arbitrary storm. This estimation is essential in the hydrologic design of water resource structures. From recent research[6,7] it appears that a unique IUH characterizing the response of a watershed does not exist but that there are possibilities of predicting the variation of the IUH satisfactorily. However, even before investigating the variation in the IUH it is necessary to investigate the methods of computation of the IUH, the limitations of these methods, and other relevant aspects. Consequently, one of the objectives of the present study is to investigate the advantages and the limitations of the computation of the impulse response functions by the transform methods. This objective may be considered as an extension of the previous work by Blank and Delleur.[6]

The computation of the impulse response functions by the transform or other methods is affected by the errors or noise in the rainfall and runoff data. The effect of noise in hydrologic data has received relatively little attention. Laurenson and O'Donnell[9] have investigated the effect of certain types of errors in the data on the accuracy of the unit hydrograph calculated by several methods, but they did not use the transform approach. In estimating the runoff given the rainfall excess and the system kernel, river basins act as low pass filters and errors in the kernel function are greatly attenuated in the calculated output. Blank, Delleur, and Giorgini[10] made a study of the error propagation due to oscillations in the kernel. By means of a perturbation analysis they found that for normal hydrologic situations an error in the kernel is reduced by a factor of 1/6 to 1/25 in the resulting output. Conversely an error in the output would be magnified in the derived kernel. Kishi[11] has investigated the error propagation in the input estimation process, namely the estimation of the input or rainfall excess, given the output and the kernel of the system. In the detection process the watershed system acts as an amplifier for the high frequencies. Consequently, in Kishi's application of linear systems analysis, relatively small errors in the output may be magnified in the calculated input. To reduce these errors, he suggested increasing the accuracy of discharge measurements.

The second objective of the present study deals with the characterization of noise and its effects on the determination of the instantaneous unit hydrographs from the effective rainfall-direct runoff data. The possibilities of reduction or elimination of the effects of noise on the IUH computations by either digital filtering or by variation of the sampling rate of the signal or by a combination of both are also investigated.

The theory of linear systems analysis by using Fourier, Laplace, and Z-transforms is reviewed first, followed by presentation of some recent results. The occurance and characterization of noise in hydrologic data are treated next, and a discussion of digital filtering in the analysis of both rural and urban hydrologic data follows.

2. THE TRANSFORM APPROACH

It is well known that for a lumped, time-invariant, linear system initially relaxed, the transform of the output is equal to the product of the transforms of the input and of the kernel function. The transformed kernel function is thus the ratio of the transforms of the output and of the input functions. The kernel function is finally obtained by inversion of its transform. The preference of one type of transform to another, for use in practice, depends substantially on the relative ease with which the numerical inversion can be performed. The theory underlying the computation of the IUH by the use of Fourier, Laplace, and Z-transforms are briefly reviewed herein.

2.1 The Fourier Transform

The Fourier transform pair is defined by the following integrals

$$f(\omega) = \int_{-\infty}^{\infty} f(t)e^{-j\omega t}dt \ , \tag{2}$$

$$f(t) = \frac{1}{2\pi}\int_{-\infty}^{\infty} f(\omega)e^{j\omega t}d\omega \ . \tag{3}$$

By taking the Fourier transform of both sides of Eq. 1, it may be shown that the convolution in the time domain is equivalent to the product of the transforms in the frequency domain:

$$Y(\omega) = X(\omega)H(\omega) \ , \tag{4a}$$

or

$$H(\omega) = \frac{Y(\omega)}{X(\omega)} \ . \tag{4b}$$

where $X(\omega)$, $Y(\omega)$ and $H(\omega)$ are the Fourier transforms of $x(t)$, $y(t)$ and $h(t)$, respectively. By expressing the exponential in the definition of the Fourier transform in terms of trigonometric functions the Fourier transform of the kernel function may be written as

$$H(\omega) = \int_{-\infty}^{\infty} h(t)[\cos \omega t - j \sin \omega t]dt \ . \tag{5}$$

Defining the real and imaginary parts of the transform by

$$R_h(\omega) = \int_{-\infty}^{\infty} h(t)\cos \omega t \, dt \ , \tag{6}$$

$$X_h(\omega) = - \int_{-\infty}^{\infty} h(t)\sin \omega t \, dt \ , \tag{7}$$

respectively, Eq. 5 becomes

$$H(\omega) = R_h(\omega) + j \, X_h(\omega) \tag{8}$$

As $h(t)$ is a real function of t, it is readily seen that $R_h(\omega)$ and $X_h(\omega)$ are, respectively, even and odd functions of ω. Similarly $R_x(\omega)$ and $R_y(\omega)$, the real parts of $X(\omega)$ and $Y(\omega)$, respectively, are even functions of ω; and $X_x(\omega)$ and $X_y(\omega)$, the imaginary parts of $X(\omega)$ and $Y(\omega)$ respectively, are odd functions of ω.

If $H(\omega)$ is known, $h(t)$ can be evaluated by means of the inversion integral, Eq. 3, which may be written as

$$\begin{aligned} h(t) &= \frac{1}{2\pi} \int_{-\infty}^{\infty} H(\omega) e^{j\omega t} d\omega \\ &= \frac{1}{2\pi} \int_{-\infty}^{\infty} [R_h(\omega) + j \, X_h(\omega)][\cos \omega t + j \sin \omega t] d\omega \\ &= \frac{1}{2\pi} \left\{ \int_{-\infty}^{\infty} [R_h(\omega) \cos \omega t - X_h(\omega)\sin \omega t] d\omega \right. \\ &\left. + j \int_{-\infty}^{\infty} [R_h(\omega)\sin \omega t + X_h(\omega)\cos \omega t] d\omega \right\} \ . \end{aligned} \tag{9}$$

As $R_h(\omega) \sin \omega t$ and $X_h(\omega) \cos \omega t$ are odd functions of ω, the last expression in Eq. 9 reduces to

$$h(t) = \frac{1}{\pi} \int_{0}^{\infty} [R_h(\omega) \cos \omega t - X_h(\omega) \sin \omega t] d\omega \tag{10}$$

The kernel function h(t) may be calculated from Eq. 10 in which $R_h(\omega)$ and $X_h(\omega)$ are, in turn, calculated with the help of Eq. 4b, or more specifically by Eqs. 11 and 12, the right hand side of which contain only the real and imaginary parts of the Fourier Transforms of the input and output functions:

$$R_h(\omega) = \frac{R_y(\omega) \cdot R_x(\omega) + X_y(\omega) \cdot X_x(\omega)}{[R_x(\omega)]^2 + [X_x(\omega)]^2} \qquad (11)$$

and

$$X_h(\omega) = \frac{X_y(\omega) \cdot R_x(\omega) - R_y(\omega) \cdot X_x(\omega)}{[R_x(\omega)]^2 + [X_x(\omega)]^2} \qquad (12)$$

2.2 The Laplace Transform

The Laplace transform pair is defined by the following two integrals:

$$H(s) = \int_0^\infty h(t)e^{-st}dt \ , \qquad (13)$$

$$h(t) = \frac{1}{2\pi j}\int_{\gamma-j\infty}^{\gamma+j\infty} H(s)e^{st}ds \ . \qquad (14)$$

The last equation is known as the Mellin integral formula. The integration is to be performed along the line Re(s) = γ. The real number γ is chosen so that it lies to the right of all the singularities of the function H(s), but is otherwise arbitrary. If the function H(s) is known in closed form, the integral of Eq. 14 can be evaluated by contour integration along the Bromwich path in the complex plane and by using Cauchy's residue theorem. Alternatively, if H(s) is known as the ratio of two polynomials such that the degree of the denominator is greater than that of the numerator, the inversion integral may be evaluated by Heaviside's expansion formula.

The difficulty usually encountered in hydrologic application of the Laplace transform to determine the IUH is that the functions H(s) are usually not known in closed form, but are known pointwise only. The classical methods of anal-

ysis, therefore, are not applicable, and it is necessary to resort to other numerical procedures for the inversion of the Laplace transform. One approach consists in reducing the Mellin integral of Eq. 14 into a Fourier integral. This method has also been called the Laplace-Gamma method, and has been discussed among others by Krylov and Skobiya[12].

Expressing the Laplace variable s as a complex frequency $s = \gamma + jq$ and considering q as the integration variable, the Mellin integral becomes

$$h(t) = \frac{1}{2\pi j} \int_{-\infty}^{\infty} e^{(\gamma + jq)t} H(\gamma + jq) j \, dq$$

$$= \frac{e^{\gamma t}}{2\pi} \int_{-\infty}^{\infty} e^{jqt} H(\gamma + jq) \, dq \quad . \tag{15}$$

Introducing the notations

$$H(\gamma + jq) = G(q) \tag{16}$$

and

$$h(t)e^{-\gamma t} = g(t) \tag{17}$$

Eq. 15 becomes

$$g(t) = \frac{1}{2\pi} \int_{-\infty}^{\infty} G(q)e^{jqt} dq \tag{18}$$

which is recognized as the inverse Fourier transform of G(q) as defined in Eq. 3.

Rewriting the Laplace transform of h(t) of Eq. 13 in terms of the complex frequency q, results in

$$H(\gamma + jq) = \int_{0}^{\infty} h(t)e^{-(\gamma+jq)t} dt \tag{19}$$

or

$$G(q) = \int_{0}^{\infty} e^{-\gamma t} h(t)e^{-jqt} dt = \int_{0}^{\infty} g(t)e^{-jqt} dt \tag{20}$$

It is immediately recognized that G(q) is the Fourier transform of g(t) and that Eqs. 18 and 20 are a Fourier transform pair.

The Fourier transform G(q) may be expressed in terms of its real and imaginary parts. Thus using the notation of Eqs. 6, 7, and 8

$$G(q) = R_g(q) + jX_g(q) \tag{21}$$

so that, by Eq. 10, the inverse of G(q) is

$$g(t) = \frac{1}{\pi}\int_o^\infty [R_g(q)\cos qt - X_g(q)\sin qt]dq \tag{22}$$

Representing the Laplace transform of the input and of the output by X(q) and Y(q), respectively, the transfer function G(q) can be written as

$$G(q) = \frac{Y(q)}{X(q)} = R_g(q) + jX_g(q) = \frac{R_y(q) + jX_y(q)}{R_x(q) + jX_x(q)} \tag{23}$$

The kernel function h(t) is then obtained by Eq. 17:

$$h(t) = \frac{e^{\gamma t}}{\pi}\int_o^\infty [R_g(q)\cos qt - X_g(q)\sin qt]dq \tag{24}$$

where

$$R_g(q) = \int_o^\infty e^{-\gamma t}\, h(t)\cos qt\, dt\ , \tag{25}$$

$$X_g(q) = -\int_o^\infty e^{-\gamma t}\, h(t)\sin qt\, dt\ . \tag{26}$$

The real and imaginary parts of the transfer function are given by equations similar to Eqs. 11 and 12 which are then introduced in the right hand side of Eq. 24 for the evaluation of h(t). It is thus seen that the inversion integral in complex plane of Eq. 14 is replaced by the integral of Eq. 24 on the real line which can be performed numerically without difficulty. It can be shown that the Eq. 24 may also be written as

$$h(t) = \frac{2e^{\gamma t}}{\pi}\int_o^\infty R_g(q)\cos qt\, dq\ , \tag{27}$$

or

$$h(t) = \frac{2e^{\gamma t}}{\pi} \int_0^\infty - X_g(q) \sin qt \, dq \tag{28}$$

The magnitude of the transfer function

$$|G(q)| = \left\{ [R_g(q)]^2 + [X_g(q)]^2 \right\}^{1/2} \tag{29}$$

may be regarded as defining a three-dimensional surface over the (γ, jq) plane. This surface has peaks to the left of the imaginary axis located at the singularities of the transfer function. To the right of these singularities the surface gradually levels towards the (γ, jq) plane. The function $|H(\omega)|$ is a cut of this surface at $\gamma = 0$. The function $|G(q)|$ is a cut of this surface for $\gamma \neq 0$. For $\gamma > 0$ the amplitudes of $G(q)$ decrease as γ increases. One may, therefore, expect that as γ increases the numerical values of the integral of Eq. 24 decrease, which are then multiplied by a proportionally larger coefficient $e^{\gamma t}/\pi$ to obtain $h(t)$. As a consequence, for large values of γ the errors in the evaluation of $h(t)$ will tend to be magnified. It is thus expected that the accuracy of the results will decrease with increasing values of γ.

2.3 The Z-Transform

The previous methods of systems analysis by the Fourier and Laplace transforms were originally developed for continuous input, output, and transfer functions. The necessary approximations were developed to extend the use of these methods to the analysis of discrete data as they are usually found in hydrology. In contradistinction, the Z-transform was developed specifically for the analysis of discrete data.

The Z-transform pair of a sequence of numbers $x(\Delta t)$, $x(2\Delta t)$, ..., $x(n\Delta t)$, is defined by

$$X(z) = \sum_{n=0}^{\infty} x(n\Delta t) z^{-n} , \tag{30}$$

$$x(n\Delta t) = \frac{1}{2\pi j} \oint X(z) z^{n-1} dz \tag{31}$$

where z is a complex variable, and the contour integral is evaluated on the unit circle.

The Z-transform may be considered as an extension of the Laplace transform. If the function f(t) is a continuous function which is zero for $t < 0$, then its discrete sampled function f*(t) and the Laplace transform of f*(t), designated by f*(s), may be written, respectively, as:

$$f^*(t) = \sum_{n=0}^{\infty} f(n\Delta t)\delta(t - n\Delta t) , \tag{32}$$

$$f^*(s) = \sum_{n=0}^{\infty} f(n\Delta t)e^{-ns\Delta t} . \tag{33}$$

Letting $Z = e^{s\Delta t}$ in Eq. 33 we retreive Eq. 30. It is seen that X(z) is given by an infinite series in powers of z^{-1}.

The Z-transform relationship between input and output sampled in synchronism is similar to the Fourier or the Laplace transform relationships for continuous functions:

$$Y(z) = H(z)X(z) \tag{34}$$

or

$$H(z) = \frac{Y(z)}{X(z)} , \tag{35}$$

where H(z) is the sampled transfer function also known as the pulsed transfer function, and X(z) and Y(z) are the Z-transforms of the input $x(n\Delta t)$ and of the output $y(n\Delta t)$, respectively. The pulsed impulse response $H(n\Delta t)$ would then be obtained by inversion of H(z). By comparing the definitions of the Laplace transform (Eq. 13) and of the Z-transform (Eq. 30), it is seen that the sampled values of the kernel function $h(n\Delta t)$ and the pulsed impulse response $H(n\Delta t)$ are related by

$$H(n\Delta T) = h(n\Delta t)/\Delta t \tag{36}$$

In practice to invert H(z) it is not necessary to use the inversion integral of Eq. 31. As H(z) is given as the ratio of two polynomials in z^{-1}, it will suffice to express the ratio in a series in powers of z^{-1} by long division for which a simple algorithm may be written. The coefficients in the series correspond to the values of the sampled function at the sampling instants. The sampled transfer function may be written, with the help of Eqs. 30 and 35, as

$$H(z) = \frac{y(\Delta t) + y(2\Delta t)z^{-1} + \ldots + y(n\Delta t)z^{-n+1}}{x(\Delta t) + x(2\Delta t)z^{-1} + \ldots + x(m\Delta t)z^{-m+1}} \tag{37}$$

since for hydrologic data x(0) = y(0). By long division Eq. 37 becomes

$$H(z) = H_1 + H_2z^{-1} + H_3z^{-2} + \ldots + H_nz^{-n} + \ldots \tag{38}$$

where

$$H_n = \left\{y(n\Delta t) - H_1x(n\Delta t) - H_2x[(n-1)\Delta t] \ldots - H_{n-1}x(2\Delta t)\right\} / x(\Delta t) \tag{39}$$

In Eq. 38 the H_n are coefficients of powers of z^{-1}, hence by Eq. 30, H_n is equal to $H(n\Delta t)$. The impulse response sampled at interval Δt is then calculated from Eq. 36 as $h(n\Delta t) = H(n\Delta t)\Delta t$.

The product of two Z-transforms in the z-plane is equivalent to the discrete convolution in the time domain. Thus if Y(z) = X(z)H(z), then

$$y(n\Delta t) = \sum_{m=0}^{n} x(m\Delta t)H(n\Delta t - m\Delta t) = \sum_{m=0}^{n} x(n\Delta t - m\Delta t)H(m\Delta t) \tag{40}$$

2.4 Computational Aspects

In practical hydrologic computation, the rainfall excess input x(t) and the direct runoff output y(t) are not given in the form of continuous functions, but the values of these functions are given at discrete time intervals. The integrals in the Fourier transform and in its inversion must therefore, be approximated by finite sums. The input and output data are assumed to be spec-

ified at the time interval Δt. For the intervals in the time domain the lower limit is taken as zero as the functions $x(t)$, $y(t)$, and $h(t)$ are zero for $t < 0$, and the upper limit is the maximum time for which the function is defined. The discretized data in the time domain do not contain significant information about Fourier components with periods less than $2\Delta t$. Consequently, it is not necessary to extend the calculation in the frequency domain for frequencies higher than $f_c = (2\Delta t)^{-1}$. This cutoff frequency is called the Nyquist frequency. The lower and upper limits of the integrals in the frequency domain are thus zero and $\omega_c = 2\pi f_c$, respectively.

If $\Delta\omega = 2\pi\Delta f$ is the frequency interval, the Fourier transforms do not contain significant information with a frequency larger than $2\Delta f$. Consequently, the largest period for which the calculation needs to be carried is $T_c = 1/(2\Delta f)$. This is a consequence of the sampling theorem in the frequency domain which states that the Fourier transform $f(\omega)$ can be uniquely reconstructed from equidistant samples, provided that $f(t) = 0$ for $|t| > T_c$. This theorem applies to the evaluation of the kernel function $h(t)$ by means of Eq. 10, as this function is bounded in the time domain. If the number of sampling points of the rainfall excess hyetograph is N_P, then the rainfall duration is $T_R = (N_P-1)\Delta t$. Likewise if the number of sampling points in the direct runoff hydrograph is N_Q, the base time of the direct runoff hydrograph is $T_Q = (N_Q-1)\Delta t$. The base time of the kernel function or of the IUH is thus $T_K = T_Q - T_R = (N_Q-N_P)\Delta t$, and the number of points in the base time of the kernel function is $N_Q - N_P + 1$. The frequency interval in the evaluation of Eq. 10 is thus $\Delta f = 1/(2T_c) = 1/[2(N_Q - N_P)\Delta t]$. If N_ω is the number of sampling points in $H(\omega)$, the number of intervals is $N_\omega - 1$ which is obtained by dividing the Nyquist frequency by the frequency interval, thus

$$N_\omega - 1 = f_c/\Delta f = 2(N_Q - N_P)\Delta t/(2\Delta t) \qquad (41)$$

or

$$N_\omega = N_Q - N_P + 1 \tag{41a}$$

It is thus seen that for the numerical evaluation of the impulsive response (Eq. 10), the frequency range from 0 to $(2\Delta t)^{-1}$ must be divided into at least $N_Q - N_P$ intervals, where N_Q and N_P are the number of sampling points in the direct runoff output, and in the rainfall excess input, respectively.

Once the kernel function $h(t)$ is evaluated it is often used in the convolution integral, Eq. 1, with the original input to regenerate the output as a verification of the correctness of the calculations. The function $h(t)$ may also be convolved with another input to predict the output. As the convolution in the time domain is equivalent to the product of the transforms in the frequency domain, the sampling theorem in the frequency domain is useful in determining the discretization requirements. The numerical evaluation of

$$y(t) = \int_0^t x(\tau)h(t - \tau)d\tau = \frac{1}{2\pi}\int_{-\infty}^{\infty} X(\omega) \cdot H(\omega)e^{j\omega t}d\omega \tag{42}$$

as a sum truncated at the Nyquist frequency can be expected to be correct for $t \leq 1/(2\Delta f)$. As it is desired to have an accurate evaluation of $y(t)$ for the whole interval 0 to T_Q, it is necessary to choose $\Delta f \leq 1/(2T_Q)$ or $\Delta\omega \leq \pi/T_Q$. Thus the number of intervals in the frequency range is $N_Q - 1$, and the number of sampling points in the integrand of Eq. 42 is N_Q, where N_Q is the desired number of sampling points in the calculated output. If the calculation is done in the time domain by a finite sum approximating the integral of Eq. 1, each of the sequences must have at least N_Q sampling points, some of which may be zeros.

The above remarks about Δt and $\Delta\omega$ and for the limits of integration regarding the Fourier transform are valid for the Laplace transform but with ω replaced by q. Additional remarks, however, are in order regarding γ. The real

part of the complex frequency must be to the right of the singularities of G(q). In practice, the locations of these are not known without assuming a mathematical model of the system. However, as the hydrologic system behaves in a manner similar to an overdamped mechanical system, it may be assumed to be stable. Therefore, γ may be taken as any positive number. In particular, for $\gamma = 0$, the Laplace-Gamma method reduces to the Fourier transform method.

Just as the Z-transform may be thought of as a discrete form of the Laplace transform, so the evaluation of the Z-transform of a finite sequence, $f(n\Delta t)$, at N points equally spaced in the z-plane at angles of $k\Omega$ radians along the unit circle, can be considered equivalent to the evaluation of the discrete Fourier transform. In fact, if in Eq. 33 the variable s is replaced by $j\omega$, and ω is discretized at intervals $\Omega = 2\pi/N\Delta t$, and the sum is carried over N terms, the right hand side of Eq. 33 becomes identical to the discrete Fourier transform which is defined by Eq. 43 and its inverse by Eq. 44.

$$F(k\Omega) = \sum_{n=0}^{N-1} f(n\Delta t)e^{-jk\Omega n\Delta t} , \tag{43}$$

$$f(n\Delta t) = \frac{1}{N} \sum_{k=0}^{N-1} F(k\Omega)e^{jk\Omega n\Delta t} \tag{44}$$

The spectral samples given by Eq. 43 may thus be imagined as vectors perpendicular to the complex z-plane and arranged along the unit circle at angular values of $k\Omega$. As a result, the product of two discrete Fourier transforms is equivalent to the discrete Fourier transform of a circular or periodic convolution of Eq. 40 and is not equivalent to a linear or aperiodic convolution as implied by Eq. 1. It thus appears that the number of sampling points in the convolution sum is equal to the number of sampling frequencies in the z-plane. Should it be desirable to extend the convolution sum further, then it

is necessary to add a sufficient number of zeros to the x or H sequences, or to both, (Eq. 40). It may now be seen that the same result applies to the evaluation of the discretized convolution integral. The number of sampling points in the finite sum approximating the convolution integral cannot exceed the number of sampling points in the sequences being convolved. If necessary, these sequences may be extended with as many zeros as necessary to avoid the periodicity effect.

2.5 Numerical Experiments

The Fourier transform method of estimating the impulse response of effective rainfall-direct runoff systems has been dealt with in detail elsewhere.[6] The experiments which are presented herein deal essentially with the Laplace and Z-transform methods. A numerical example has been selected so that the computational aspects of the Laplace and Z-transforms can be demonstrated without bringing the effects of noise on the computations.

The example chosen for the numerical experiments was suggested by Dooge[13] but was modified so that it would satisfy the continuity equation. The shapes of the input, output, and kernel functions are similar to those found in typical hydrologic problems. The input function is given by

$$x(t) = t(1 - t)e^{1-t}(e^{8} - 41) \quad ; \quad 0 \leq t \leq 1 \tag{45}$$

the output function is

$$y(t) = \begin{cases} e^{9-t}\, t^3(2 - t)/12 + e^{1-t}\,(t^2 + 3t + 4) - e(4 - t) & ; \quad 0 \leq t < 1 \quad (46a) \\ e^{9-t}\,(2t - 1)/12 + (11 - 3t) - e(4 - t) & ; \quad 1 \leq t < 8 \quad (46b) \\ (e^{9-t}/12)[12t^2 - 130t + 335 - (t - 8)^2 \\ \qquad (152 - 14t - t^2)] + (11 - 3t) & ; \quad 8 \leq t \leq 9 \quad (46c) \end{cases}$$

and the kernel function is given by

$$h(t) = t(e^{8-t} - 1)/(e^{8} - 41) \quad ; \quad 0 \leq t \leq 8 \qquad (47)$$

The Laplace transforms of the output and input functions were first computed by using the finite difference form of Eq. 13, with $s = \gamma + jq$ and in which the frequency q was varied from zero to q_m. By using the real and imaginary parts of the output and input transforms in Eq. 11 and 12 (with ω replaced by q), the real and imaginary parts of the transfer function were computed, which were in turn substituted back into Eq. 24 to obtain the response function h(t). The response function was convolved with the input to regenerate the outflow hydrograph. The numerical experiments were conducted to determine the effect of changes in γ (Eq. 24) and in q_m on the computational scheme. The following notation is used in the presentation of results:

X(t) - Given input - Theoretical - (Eq. 45)

Y(t) - Given output - Theoretical - (Eq. 46a - 46c)

Amplitude - (Eq. 29)

H(t) - Theoretical impulse response, Eq. 47

H1(t) - Response function computed by using Eq. 27

H2(t) - Response function computed by using Eq. 28

H3(t) - Response function calculated by Fourier Transform, Eq. 10

H4(t) - Response function computed by using Eq. 24

Z1(t) - Output regenerated by convolving the input with H1(t) - (Eq. 1)

Z2(t) - Output regenerated by convolving the input with H2(t) - (Eq. 1)

Z3(t) - Output regenerated by convolving the input with H3(t) - (Eq. 1)

Z4(t) - Output regenerated by convolving the input with H4(t) - (Eq. 1)

q_m - Truncation frequency in numerical evaluation of Eq. 24, 27, 28

γ - A parameter in Eq. 24, 27, 28

2.5.1 Changes in the γ Values

The effects of changing γ on the evaluation of h(t) are shown in Fig. 1. The results for the Fourier transform (γ = 0) and for the Laplace transform (γ = 0.1, 0.3, 0.6, and 1.0) are shown in the figure. The ΔT value used for discretizing the input and output data was equal to 0.1, and the truncation frequency, $q_m = \pi/0.1 = 10\pi$, which is the Nyquist frequency, was used in all the cases. The range (0, q_m) was divided into N_Q intervals where N_Q is the number of points defined on the outflow hydrograph. The results are essentially the same for all the γ values tested. However, if larger γ values are selected, the errors in the computation of integrals in Eq. 24, 27, and 28, increase with an increasing value of γ.

2.5.2 Effect of Negative γ Values on Computations

The effect of negative γ values on the behavior of the computed IUH is shown in Figure 2. Although the γ values in the Laplace-Gamma method are traditionally selected to be on the positive side of the axis in the complex plane, the only restriction on the selection of the γ values is that they should be to the right of the singularities. However, the negative γ values have the apparent advantage that they do not amplify the errors in the integrals as positive γ values tend to do, and, consequently, this experiment was undertaken. The results of the experiments indicate that the negative γ values introduce higher oscillations in the amplitude values than the corresponding positive γ values. The response functions and the regenerated hydrographs differ negligibly from those computed by using positive γ values shown in Figure 1.

2.5.3 Effects of Varying the Discretization Rate

An increase of the time-step Δt results in a decrease of Nyquist frequency which is used as the truncation frequency in the numerical evaluation of the

integrations in the frequency domain. The effect of changing the discretization rate is shown in Figure 3.

In Figures 3a and 3b are shown the Fourier amplitude spectra, X_1, of y(t) and X_2 of x(t) versus the angular frequency, ω, for three values of the time step Δt, calculated in each case for angular frequencies up to the Nyquist frequency, $\omega_c = \pi/\Delta t$ radians per unit of time. The amplitude spectra of the input are shown to differ for the several values of Δt whereas those of the output do not. It appears that for all values of the time step the amplitude spectra of the output have decayed to zero at an angular frequency of approximately 5π, whereas the amplitude spectra of the input still have very significant values at that frequency, but remain close to zero for angular frequencies larger than approximately 12π.

2.5.4 Stability of the Kernel Functions

In the system identification, as the transfer function is obtained from $H(\omega) = Y(\omega)/X(\omega)$, small values of $X(\omega)$ at frequencies where $Y(\omega)$ is nonzero may result in large values of $H(\omega)$ at these frequencies. When this situation occurs spurious spikes appear in the transfer function in the frequency domain and are translated in the form of oscillations in the kernel function in the time domain. These oscillations may be reduced by increasing the size of the time step Δt. However, Δt may not be increased indefinitely, as it is necessary to maintain a spectrum decaying to zero at $\omega \leq \omega_c$, and as Δt must be small enough to maintain the desired resolution in the time domain. Resolution in the time domain refers to the duration of the narrowest detail which is desired to be observed in the time functions, x(t), y(t), and h(t).

In Figures 3c and 3d the amplitude spectra of the direct runoff X_1 and of the rainfall excess X_2, respectively are shown for values of Δt of 0.5 hr, 1 hr, and 2 hr for the storm of June 22, 1960, on the Muscatatuck River

near Deputy, Indiana. [The sources of these data used in the present study and the procedures adopted to obtain the effective rainfall and direct runoff are described in detail elsewhere[6,7].] The amplitude spectra of the input, X_2, reach values of almost zero at an angular frequency of approximately 0.5, and oscillate considerably thereafter without reaching zero even at an angular frequency of 6. The amplitude spectra of the output, X_1, gradually reach values near zero at an angular frequency of about 0.5. Consequently, the transfer function $H(\omega) = Y(\omega)/X(\omega)$ attains high values at the frequency of 0.5 resulting in a spike in its amplitude spectrum X_3 at that frequency as shown in Figure 3e. The spikes in the amplitude spectra of the transfer function in the frequency domain are translated into oscillations of the kernel function in the time domain, as shown in Figure 3f. The spurious spike in the transfer function and the consequent oscillations in the kernel function may be eliminated by taking a larger value of Δt. For Δt = 2 hrs the spurious spike has been attenuated considerably. However, in this particular example, the input transform with Δt = 2 hrs has not reached a small enough value at the Nyquist frequency to use this method exclusively for the elimination of the effect of the noise.

2.5.5 Effects of Varying the Truncation Frequency

The truncation frequency is usually taken as the Nyquist frequency $\omega_c = \pi/\Delta t$. Taking the truncation frequency larger than ω_c will lead to erroneous results due to aliasing. However, it is permissible to select a truncation frequency $q_m < \omega_c$ if the amplitude spectrum decays gradually reaching a negligible value at a frequency q_m.

The results of varying the truncation frequency, q_m are shown in Figure 4. The minimum and the maximum values of the truncation frequency used in the experiment were half and twice the Nyquist frequency or 5π and 20π, re-

spectively. It may be observed in Figure 1 that the amplitude spectrum oscillates around zero for frequencies larger than about 3π. It appears, therefore, that the frequencies between 3π and 10π contain very little information, if any. For this reason the integration between 3π and 10π does not improve the results; on the contrary, it may bring in noise which may be present in the frequency band. This conclusion is verified by the fact that the kernel values obtained for $q_m = 10\pi$ have greater discontinuities at $t = 1$ and 8 (Figure 1) than the corresponding computations shown in Figures 4b and 4c. The value of $q_m = 20\pi$, or twice the Nyquist frequency, obviously yields erroneous results, as frequencies higher than the Nyquist frequency do not contain any information. The results shown in Figures 4e and 4f show the instabilities introduced by these higher frequencies.

2.5.6 Application of Laplace Transform Method to Field Data

The Laplace transform method of determination of the IUH, which was discussed earlier was tested by using the field data. The watersheds are identified in Table 1. The IUH obtained by the Fourier transform method are also shown for all the cases. For all the cases, the value of γ used was 0.1, and the cutoff frequency q_m was $\pi/\Delta t$. The results shown in Figure 5 substantiate the fact that the Laplace and the Fourier transform methods yield identical results.

2.5.7 The Z-Transform Computations

The Z-transform method can be shown to be equivalent to the so called "Direct Method".[6] Previous results of the computations made by using the direct method and the theoretical example mentioned earlier indicates that there is no difference in the response functions obtained by the direct method and the Fourier transform method (Ref. 6, page 61). Some results obtained by the use of the Z-transform method on field data are shown in Figure 6. These results

TABLE I

NAME	WATERSHED NUMBER	STORM NUMBER	DATA OF STORM	AREA OF WATERSHED (SQ. Mi.)	RURAL OR URBAN
Ross Ade Drain W. Lafayette, Ind.	1	3	10/15/67	0455	Urban
Ross Ade Drain W. Lafayette, Ind.		4	8/20/67	0455	Urban
Bean Blossom Creek at Bean Blossom, Ind.	3	14	4/25/61	14.60	Rural
Mississinewa River near Ridgeville, Ind.	6	15	1/16/53	130.0	Rural
Mississinewa River near Ridgeville, Ind.	6	23	2/17/56	130.0	Rural
White Lick Creek at Mooresville, Inc.	21	11	5/21/62	212	Rural
Salamonie River at Portland, Ind.	35	21	9/ 1/61	86	Rural
Carpenter Creek near Egypt, Ind.	40	11	6/22/60	48.10	Rural
Carpenter Creek near Egypt, Ind.	40	13	5/16/60	48.10	Rural
Eagle Creek near Zionville, Ind.	51	11	7/ 3/60	102	Rural
Muscatatuck River	57	8	6/22/60	296	Rural

are further discussed in the next section.

2.5.8 Relative Merits of the Several Transforms

In light of the above experiments the following general comments appear to be in order.

In general, the kernel functions H4(t) using the sine and cosine inverse Laplace transform were more accurate and more stable than either the sine or the cosine inverse Laplace transforms, H1(t) and H2(t), respectively, for all the t values which were considered. When there is a positive outflow or inflow value at t = 0, the results of computation of the sine inverse Laplace transform, H2(t), will be erroneous as H2(t) will always be forced to be equal to zero at t = 0, according to Eq. 28. The kernel function H3(t) using the sine and cosine inverse Fourier transforms, (Eq. 10), is a particular case of H4(t) with $\gamma = 0$ and gives consistently reliable results. These conclusions were also borne out by the analysis of field data.

The Z-transform results for two different watersheds are shown in Figure 6. The instantaneous unit hydrographs obtained by both methods are essentially the same. The Z-transform method has the advantage that the corresponding algorithm to find the IUH is much simpler and shorter than those for either the Fourier or the Laplace transforms. As a result the computer time for the Z-transform calculations is considerably less than for the other methods, by a factor of 1/10 approximately.

It could have been anticipated that the results by the Z-transform would be less accurate than those by the Fourier or Laplace transform as each value of the sampled transfer function H_n depends on the previous values (see Eq. 39), whereas in the Fourier and Laplace methods, each value of the transfer function is calculated independently and depends on all the values of the input and output functions. At least with the 15 place accuracy of the computer used (CDC 6500) there was no discernible propagation of error by the Z-transform method.

3. NOISE IN HYDROLOGIC DATA

In the determination of the impulse response functions by the transform methods the noise in the input and output data plays a significant role. Essentially, if the data are noisy, the impulse response functions may exhibit an oscillatory behavior.[6] In the previous discussion of the selection of truncation frequency (2.5.5) it has been pointed out that spurious peaks occur in the amplitude spectrum of the response function partly as a result of the nature of the computations. The intensity of these sprulous peaks is intimately related to the ordinate spacing in the data (Figure 3). As the oscillatory behavior of impulse response functions is related to both the errors in the data and to ordinate spacing it was decided to investigate both of these aspects.

3.1 Error Noise in Hydrologic Data

Errors in hydrologic data can result from the following sources: 1) errors in reading stage hydrographs, 2) errors inherent in the rating table, 3) errors associated with the method used in base-flow separation, 4) errors resulting from an inadequate network of precipitation stations and 5) error in the method of determining the rainfall excess. While the errors associated with reading the stage hydrograph can be estimated, at present no accurate assessment can be made of the other errors involved. It would appear that the errors resulting from an inadequate network of precipitation stations may be predominant. Even on large fronts the storm structure usually consists of trains of more or less parallel agglomeration of convective cells. As a result the precipitation changes rapidly in time and space over a watershed. The point rainfall measurement with a density of one rain gage per 250 square miles, as is the case in Indiana, is unlikely to be representative of the actual rainfall on the watershed. On the contrary, the runoff is eventually collected at a single point, the mouth of the watershed. At the gaging stations maintained

by the U.S. Geological Survey the rating curves are checked periodically and the discharge data are usually of very good quality. It could, therefore, be reasonably assumed that the runoff is reasonably noise-free compared to the rainfall. Based on this assumption a computational scheme was set up to measure the noise in the rainfall data.

3.1.1 Estimation of Noise Attributable to Rainfall Excess Data

The direct runoff data were used as the signal input to two parallel computational branches, as shown in Figure 7. One branch consisted of the previously derived watershed system but operating in the detection mode and followed by an attenuator. In the second branch the attenuator precedes the watershed system. In the first branch the input into the attenuator, $g_1(t)$, has a large signal to noise ratio, and after passing through the attenuator the amount of noise in the output of the first branch will be very small. On the contrary, most of the noise generated by the watershed system in the detection mode will be contained in the output $g_2(t)$ of the second branch. The difference between the signals $g_1(t)$ and $g_2(t)$ is a measure of the noise created by the watershed system operated in the detection mode. It is then possible to estimate the spectrum of the noise so measured.

Kishi[11] has stated that the watershed system in the detection process amplified high frequency noise in the runoff measurements that may be due to the effect of turbulence and flow unsteadiness on the current meters. In the data used in this study, the flow rates were obtained from stage measurements converted to discharges by stage-discharge rating curves. These curves were obtained by averaging numerous flow meter point measurements and the turbulence induced errors should be essentially eliminated. It would then appear that the noise measured by the computational scheme of Figure 7 is primarily the noise embedded in the kernel function through the rainfall data.

Figure 8 shows the probability distribution of the noise of combined data for three storms. The probability distribution is approximately symmetric about the origin.

The effect of noise in the determination of the impulse response can be alternatively investigated by considering the action of the watershed. In the runoff prediction the watershed system acts as a low pass filter. This may now be verified as follows. Let us assume that the true input signal $x_o(t)$ is contaminated by a noise $e(t)$ so that the observed signal is

$$x(t) = x_o(t) + e(t) \tag{48}$$

Let us approximate the probability distribution of the noise of Figure 8 by a uniform distribution with a frequency given by a constant $1/Eo$ for $\frac{-Eo}{2} \leq e \leq \frac{Eo}{2}$, and zero elsewhere. Then the variance of the error is

$$\text{Var } e(t) = \int_{-Eo/2}^{Eo/2} e^2 \cdot \frac{1}{Eo}\, de = \frac{Eo^2}{12} \tag{49}$$

If the system were subject to the noise only, the output would be

$$f(t) = \int_o^t e(t)\, h(t-\tau)d\tau \tag{50}$$

and the variance of the output signal would be

$$\sigma_f^2 = \frac{Eo^2}{12} \int_o^\infty h^2(t)dt \tag{51}$$

As for hydrologic system $\int_o^\infty h(t)dt = 1$, it follows that $\int_o^\infty h^2(t)dt < 1$ and the variance of the output is less than the variance of the input noise. For this reason, noise in the input data or in the kernel function is usually masked in the convolution operation yielding smooth output functions.

Blank, Delleur, and Giorgini[10] found that an error in the kernel is reduced by a factor varying from 1/6 to 1/25 in the resulting output obtained by convolution. Conversely an error in the output would be magnified in the derived kernel. This shows that the kernel function is very sensitive to errors in the

output data. Numerical experiments by Blank and Delleur,[6] in which known smooth input and output functions were perturbed by a random noise with an amplitude less than 10% of the maximum signal, resulted in strong oscillations in the kernel function. The amplitude of these oscillations reached 8 times the maximum amplitude of the undisturbed kernel. It is thus apparent that the kernel functions are very sensitive to noise both in the input and output functions. This result justifies the practice of either smoothing the kernel function or of attempting to eliminate the noise in the data. Further observation of the results showed that the frequency of the oscillations in the kernel function was close to the Nyquist frequency. This indicated that the noise was principally in the high frequency range, and that it could be greatly attenuated by means of a low-pass filter.

3.2 Digital Filters

A filter may be described as a linear system which has a frequency response with a specified amplitude, $|W(\omega)|$, and phase, $\theta(\omega)$, in the frequency domain. If the amplitude is a constant, generally unity, for $\omega < \omega_c$, and is small for $\omega > \omega_c$, then the filter is called a low-pass filter and ω_c is the cutoff frequency. The impulsive response, $w(t)$, of the filter is obviously the inverse Fourier transform of its frequency response function $W(\omega)$. For the continuous filter the relationship between the input and the output or filtered result is

$$y(t) = \int_0^\infty w(t)x(t-\tau)d\tau \tag{52}$$

such that

$$W(\omega) = |W(\omega)|e^{-j\theta(\omega)} \tag{53}$$

has the desired amplitude and phase characteristics. The functions $w(t)$ and $W(\omega)$ are called the data window and spectral window, respectively, according

to the terminology introduced by Blackman and Tukey[14]. For digital filters the convolution integral is replaced by a convolution sum

$$y_t = \sum_{i=-m}^{n} w_i x_{t-i} \tag{54}$$

Filters of this type (Eq. 54) are called moving averages, and are non-recursive as they do not have any feedback. The filters used in this study are of this type. For discrete filters, the frequency response in terms of $f = \omega/2\pi$ is given by

$$W(k\Delta f) = \sum_{i=-m}^{m} w_i \cos(2\pi k\Delta f i\Delta t) - J \sum_{i=-m}^{m} w_i \sin(2\pi k\Delta f i\Delta t) \tag{55}$$

which is the counterpart of Eq. 5 for continuous systems. Note that the phase can be made equal to zero by taking $w_i = w_{-i}$, when the frequency response reduces to

$$W(k\Delta f) = w_o + 2 \sum_{i=1}^{m} w_i \cos(2\pi k\Delta f i\Delta t) \quad - \frac{1}{2\Delta t} \leq k\Delta f < \frac{1}{2\Delta t} \tag{56}$$

The Tukey window[14] (sometimes called Hanning) is a low pass filter often used in spectral analysis. The Tukey data and spectral windows are given by

$$w_i = \frac{1}{2}\left(1 + \cos\frac{\pi i}{m}\right) \tag{57}$$

$$W(k\Delta f) = m\Delta t\left(\frac{\sin 2\pi k\Delta f m\Delta t}{2\pi k\Delta f m\Delta t}\right) \frac{1}{1-(2\pi k\Delta f m\Delta t)^2} \tag{58}$$

Alavi and Jenkins[15] modified the Tukey window to obtain a high-pass filter. Its data and spectral windows are given by

$$w_o = 1 - \frac{1}{m+1} \tag{59}$$

$$w_i = w_{-i} = -\frac{1}{m+1}\left[\frac{1}{2} + \frac{1}{2}\cos\frac{i\pi}{m+1}\right], \quad i = 1, \ldots m \tag{60}$$

$$W(f) = w_o + 2 \sum_{i=1}^{m} w_i \cos 2\pi k\Delta f i\Delta t \tag{61}$$

For the filtering of the hydrologic data, a low pass filter is needed with the cut-off frequency near the Nyquist frequency. Delleur[16] obtained this type of filter by translation of the frequency response function in the frequency domain

$$W'(f) = W(0.5 - f) = w_o + 2 \sum_{i=1}^{m} (-1)^i w_i \cos 2\pi f i \Delta t \ . \qquad (62)$$

It is seen that the low pass filter is simply obtained by multiplying the weight coefficients w_i by $(-1)^i$. This filter will be called the modified Jenkins filter, MJF, and its frequency response is shown in Figure 9.

A refinement of the Tukey window was suggested by Blackman[14]. The corresponding discrete high pass filter has the following data and spectral windows:

$$w_o = \frac{0.16\ m}{m + 1} \qquad (63)$$

$$w_i = w_{-i} = -\frac{1}{m+1}\left(0.42 + 0.50 \cos \frac{i\pi}{m+1} + 0.08 \cos \frac{2i\pi}{m+1}\right)$$

$$i = 1, 2, \ldots m \qquad (64)$$

$$W(f) = w_o + 2 \sum_{i=1}^{m} w_i \cos 2\pi f i \Delta t$$

As before a low pass filter with cutoff near the Nyquist frequency may be obtained by replacing w_i by $(-1)^i w_i$. This filter will be called the modified Blackman filter, MBF, and its frequency response is also shown in Figure 9.

3.3 Numerical Experiments

3.3.1 Effect of Filters on the Data

The MJF and the MBF were applied to effective rainfall and direct runoff data from some Indiana watersheds. The determination of the effective rainfall and of the direct runoff for rural and urban watersheds are discussed in Refs. 6 and 7, respectively. Figure 10 illustrates the effect of the MJF and the MBF on the data. When the data are filtered, 2m data points, m each at the beginning and at the end, are lost. If the number of data points is

large, such as in a hydrograph, this effect is not serious. If it is small, as in a hyetograph, then the volume of rainfall is drastically reduced and is not the same as the volume of runoff. This effect is illustrated in Figure 10 which shows a comparison of original and filtered effective rainfall and direct runoff data for different values of m. In order to circumvent this situation, the volumes of the original rainfall and runoff were computed and the ordinates of the filtered hydrograph and hyetograph were, respectively, multiplied by the following ratios: (volume of the original hydrograph/volume of the filtered hydrograph) and (volume of the original hyetograph/volume of the filtered hyetograph). The hydrographs and hyetographs resulting from this procedure are referred to as "adjusted" data. The adjusted rainfall and runoff data are also shown in Figure 10. Between the two filters, it can be seen that the MJF causes a lesser distortion of the data than the MBF.

3.3.2 Effect of Filtering on Noise Spectrum

The effects of filtering the data on the noise spectra are indicated in Figure 11. Figures 11a and 11b show the effect of filtering on the estimated spectra of the noise attributed to the input and calculated by the scheme shown in Figure 7. The input and output data used to evaluate $H(\omega)$ were filtered using filters with values for m (designated by M on the figures) of 1 and 5 in 11b and 11c respectively. The estimated spectra for various attenuation factors are also shown in Figure 11c. From Figure 11c it is apparent that the value of the attenuation is immaterial, at least within the bounds tested. The effectiveness of the filter is shown in the reduction of the spectral values obtained from filtered data with M = 1 shown in Figure 11b compared to the spectral values obtained with unfiltered values shown in Figure 11a. Comparing the noise spectra shown in Figures 11b and 11c it appears that an increase in the value of M from 1 to 5 shifts the filter cutoff frequency towards the Nyquist

frequency and beyond the frequency of the spike in the amplitude spectrum of the transfer function. This reduces the effectiveness of the filtering with the result that the spectral values are of the same order of magnitude as with the unfiltered data.

3.3.3 Combined Effect of Ordinate Spacing Variation and Filtering

The effect of variation of both the ordinate spacing and the filtering on the kernel oscillations is illustrated in Figure 12. The kernel functions were computed for data with the original ordinate spacing Δt, and for ordinate spacings $2\Delta t$ and $(\Delta t/2)$. In Figure 12a the variation of amplitudes of the kernel functions in the frequency domain, and the corresponding kernel functions are shown for unfiltered data. It can be seen that the kernel oscillations are very predominant for kernel functions obtained with data of spacing Δt and $\Delta t/2$ whereas they are much less evident for the kernel functions obtained with data of spacing $2\Delta t$. For the data with spacing Δt and $\Delta t/2$ we can also notice prominant spikes in the amplitudes of the kernel function around a frequency of 1.57.

In Figure 12b are shown results similar to those described above but which were obtained after the data were filtered (MJF, M = 1). The kernel for data with spacing $2\Delta t$ is devoid of any oscillations whereas the kernels for the other two cases still exhibit considerable oscillations. In fact, the spike in the amplitude spectrum around the frequency of 1.57 are more predominant than those observed in Figure 12a.

With M = 2, (Figure 12c) the kernel which was obtained from data of spacing $2\Delta t$ is very smooth, and the kernels obtained from the data of Δt and $(\Delta t/2)$ are also smoother than the corresponding kernels in Figures 12a and 12b.

In Figure 12d the order of the filter is 3, and it can be seen that the kernel functions obtained from all the data are smoother than those shown in

Figure 12c. This smoothing out, however, may not be consistent and some times the kernel oscillations may increase. These increased oscillations can be attributed to the extreme distortions that the input data undergoes when short sequences of rainfall data are filtered (Figure 10).

From the results presented in Figure 12 an obvious question, "if the kernel oscillations are mostly eliminated by increased ordinate spacing, what is the practicality of filtering?" arises. Although in the example in Figure 12, the kernel oscillations are much reduced by doubling the ordinate spacing, this does not occur consistently. The increase in the time interval is limited by the requirement that the transfer function should tend to zero as the Nyquist frequency is approached.

From the foregoing it is obvious that the oscillations in the response functions are due to a combination of effects due to the sampling rate and due to the errors in the data. Thus the combination of the proper ordinate spacing and of filtering yields the smoothest kernel functions.

3.3.4 Filtering only the Input, only the Output or both Input and Output

The typical results of filtering (MJF, M = 1) only the input, the output or both the input and output are shown in Figure 13. As seen in Figures 13a and 13b, filtering the input and the input and output affects the kernel function whereas filtering the output only does not affect the kernel function oscillations at all. The effect of increasing the ordinate spacing and filtering (MJF, M = 1) only the input, or the output etc. are also shown in Figure 13. The ordinate spacing itself has smoothed the response functions considerably whereas filtering only the input or input and output, has improved the results only slightly in comparison with filtering only the output.

3.3.5 Effect of Filter Order

The effects on the kernel function of filtering and adjusting only the input or only the output or both the input and output, as well as the effects of changes in m on the kernel function behavior are shown in Figure 14. As it can be seen that for m = 1 (Figure 14a) filtering only the input will not smooth the kernel function but has the adverse effect of increasing the oscillations; whereas filtering only the output or both the input and output eliminates (Figure 14b, 14c) the oscillations to a large extent. With m = 7, filtering only the input (Figure 14d), or both the input and the output (Figure 14f) eliminates the oscillations, with the input filtering results being better. Filtering only the output (Figure 14e), on the other hand, is not as effective. As the use of higher order filters entails increasing distortion of data, and as the advantages to be gained by the use of higher order filters is not always significant, it can be concluded that the filter of lowest order which performs satisfactorily is to be selected.

3.3.6 Results Obtained With the Modified Blackman Filter

Typical results of filtering only the input, or the output, or both input and output by using the Modified Blackman filter (MBF) are shown in Figures 15a-15c. The inefficiency of the Blackman filter is clearly brought out in comparison of Figures 14a and 15a. The oscillations in Figure 15a are larger than those in Figure 14a. The kernel function after it is filtered by using the MBF in 15a has greater oscillations than the unfiltered kernel function. The reason for this behavior is obvious. As mentioned earlier, if the noise in the data is not filtered, as it may happen due to the characteristics of the low order Blackman filter (Figure 9, m = 1) and if the data are distorted by the filtering operation (Figure 10), then the kernel function oscillations will actually be increased. This is the case in Figure 15a. In all the numer-

ical experiments which were performed, the Jenkins filter was usually better than the Blackman filter.

3.3.7 Filtering the Kernel Function in the Time Domain

In many instances when the data are small, filtering the original data may present considerable problems. This is especially true for rainfall data for which only a few values may be available for a storm. In such instances it is preferable to obtain the response functions and filter them to eliminate their oscillations. The efficiency of this approach is illustrated in Figure 16. The response functions in these instances have been smoothed out by the use of a filter of order (m) one. Consequently, for situations where the input and outputs are small filtering the response functions can be used as an effective method of reducing the kernel function oscillations.

3.3.8 Filtering the Transfer Function in the Frequency Domain

The need for filtering is usually apparent from the appearance of the amplitude spectrum of the transfer function as a spike in the transfer function in the frequency domain will be translated into oscillations of the kernel function in the time domain. The cutoff frequency of the filter selected to eliminate these oscillations should be slightly lower than the frequency of the spurious peak in the transfer function. Because of the necessity of examining the amplitude spectrum of the transfer function for the selection of the filter it may be advantageous to perform the filtering operation in the frequency domain rather than in the time domain.

The advantages of filtering the transfer function in the frequency domain are the following. First, the numerical convolution of Equation 54 in the time domain is replaced in the frequency domain by a multiplication (by the filter transfer function), thus simplifying the computational procedure. Furthermore, there is no loss of information, as no data are "lost" as is unavoidably the

case with non-recursive filters in the time domain.

Figure 17 shows the results of filtering in the frequency domain with decreasing cutoff frequencies using the MJF transfer function (Equation 62) with m = 2 and m = 1, and also using the Tukey window (Equation 58) with m = 1 and Δt = 1/4 hour. It should be remembered that for the MJF the cutoff frequency approaches the Nyquist frequency as m increases, whereas for the Tukey window the cutoff frequency varies inversely with the parameter $m\Delta t$. It may be observed that with the MJF a better smoothing of the kernel function is obtained with m = 1 than with m = 2, because of the lower cutoff frequency of the former filter, thus eliminating more of the high frequency information in the transfer function. The cutoff frequency of the Tukey window being substantially lower, more of the high frequency information is eliminated with the result that the regenerated hydrograph does not match exactly the observed hydrograph close to the peak.

3.3.9 Examples from Small Urban Watersheds

Figures 18a and 18b illustrate the use of filtering and increasing the ordinate spacing on some urban hydrologic data in which rather severe kernel oscillations were observed. The data are acquired at 1 minute intervals and they were magnified while recording also. The description of the watersheds and of their instrumentation may be found in Reference 7. The response functions, just as the hydrographs themselves, have extremely short times of rise and comparatively long recession periods. In these cases not only the errors in the data but also the rainfall synchronization with runoff has been observed to give rise to oscillations in the kernel functions. The response function obtained for the time interval of 1 min. has very violent oscillations which may be attributed to the two sources of error mentioned earlier. With time intervals of 2 min. the oscillations have diminished considerably. The high frequency oscillations which are prevalent for Δt = 1 min. are reduced to low frequency os-

cillations, which have not been completely removed. The filter efficiency has not improved with increasing orders but for the results presented in Figure 18a, it has in fact deteriorated.

4. CONCLUSIONS

1. The transform approach in the identification of effective rainfall - direct runoff systems is general, and computationally simple. Of the three approaches, the Fourier, Laplace, and the Z-transform - studied, the Z-transform is the simplest and the fastest and computationally as accurate as the other two methods.

2. Oscillations are sometimes observed in the kernel function independently of the method used. These are conveniently explained in terms of the Fourier transform which is related to the other two transform methods.

3. The oscillations in the kernel function are in general due to spurious peaks in the transfer function. As the transfer function is the ratio of the transforms of the output and of the input, the transfer function may exhibit peaks at those frequencies where valleys occur in the input transform.

4. These instabilities may be introduced by noise in the input and output data or by the computational procedure or a combination of both.

5. A high resolution in the time domain, namely a large discretization rate (i.e. a small time interval) may result in a Nyquist frequency higher than the maximum frequency for which significant information exists and may also result in possible instabilities in the transforms particularly in the higher frequencies.

6. The amplitude spectrum of the transfer function is useful in determining the frequency at which an instability occurs, which may serve as a guide in the relation of the method to control the spurious oscillations in the kernel function.

7. The oscillations in the kernel function may be controlled by a) increasing the time step (which decreases the Nyquist frequency); b) by truncating the integrations in the frequency domain at a frequency lower than

the Nyquist frequency, provided that the amplitude spectrum of the transfer function has reached a negligible value at the truncation frequency; c) by filtering the input data or the input and output data, if sufficient input data are available to avoid an excessive distortion of the input hyetograph. The filter cutoff frequency should be less than the frequency of the spurious peak in the amplitude spectrum of the transfer function obtained with unfiltered data. It is desirable to adjust the filtered data to preserve the conservation of mass. This is done by multiplying the filtered hydrograph and hyetograph, respectively, by the ratios: (volume of original hydrograph/volume of filtered hydrograph) and (volume of original hyetograph/volume of filtered hyetograph); d) by filtering the kernel function. This method is useful to avoid the distortion that would occur in the filtered hyetograph if the sequence of input data is particularly short, or if the cutoff frequency is fairly high, i.e. m relatively large.; e) by smoothing the transfer function. This operation is done in the frequency domain and has the advantages of being computationally simple without loss of information as is the case in the time domain filtering.; f) a combination of time step increase and filtering.

8. A method was given to estimate the noise contained in the input hyetograph under the assumption that the runoff data are reasonably noise free.

9. For the data tested the input noise spectrum was approximately similar to that of a white noise, and probability distribution of the noise appears to be symmetric.

LIST OF REFERENCES

1. Sherman, L. K. "Stream Flow from Rainfall by Unit-Graph Method", Engineering News-Record, 108, 501-505, 1932.

2. Dooge, J. C. I. "A General Theory of the Unit Hydrograph", Journal of Geophysical Research, Vol. 64, 241-256, 1959.

3. Levi, E., and Valdes, R. "A Method for Direct Analysis of Hydrograph", Journal of Hydrology, Vol. 2, p. 182-190, 1964.

4. Diskin, M. H. "A Basic Study of the Linearity of the Rainfall-Runoff Process in Watersheds", Ph.D. Thesis, University of Illinois, Urbana, Illinois, 1964.

5. Yamaoka, I., and Fujita, M. "Evaluation of Simulation Models for River Runoff through Nyquist Plots", Proceedings, XIIIth Congress IAHR, Kyoto, 1969, Vol. 1, p. 171-180.

6. Blank, D., and Delleur, J. W. "A Program for Estimating Runoff from Indiana Watersheds - Part I. Linear System Analysis in Surface Hydrology, and its Application to Indiana Watersheds", Purdue University, Water Resources Research Center, Tech. Rept. No. 4.

7. Sarma, P. B. S., Delleur, J. W., and Rao, A. R. "A Program in Urban Hydrology - Part II. An Evaluation of Rainfall-Runoff Models for Small Urbanized Watersheds and the Effect of Urbanization on Runoff", Purdue University, Water Resources Research Center, Tech. Rept. No. 9, Oct. 1969.

8. Chow, Ven Te "Runoff", Section 14 in "Handbook of Applied Hydrology", Ven Te Chow, Editor, McGraw-Hill, 1964.

9. Laurenson, E. M., and O'Donnell, T. "Data Error Effects in Unit Hydrograph Derivation", Journal of the Hydraulics Division, ASCE, Vol. 95, No. HY6, Nov. 1969.

10. Blank, D., Delleur, J. W., and Giorgini, A. "Oscillatory Kernel Functions in Linear Hydrologic Models", Water Resources Research to be published, October 1971.

11. Kishi, T. "Effect of An Error in Discharge Measurements on the Detection Process in Runoff Systems Analysis", US-Japan Bi-Lateral Seminar in Hydrology, Honolulu, January 1971.

12. Krylov, V. I. and Skoblya, N. S. "Handbook of Numerical Inversion of Laplace Transforms", Israel Program for Scientific Translations, 1969, (Translated from Russian).

13. Dooge, J. C. I. "Analysis of Linear Systems by Means of Laguerre Functions", Journal SIAM (Control) 2(3), p. 396-408, 1965.

14. Blackman, R. B., and Tukey, J. W. "The Measurement of Power Spectra", Dover, 1959.

15. Alavi, A. S., and Jenkins, G. M. "An Example of Digital Filtering", Applied Statistics, Vol. 14, p. 70, 1965.

16. Delleur, J. W. "Réflexions sur l'Analyse Spectrale", Laboratoire National d'Hydraulique, Chatou, France, Rept. ST22, Jul. 1969.

17. Delleur, J. W. and Rao, R. A. "Linear Systems Analysis in Hydrology - The Transform Approach, the Kernel Oscillations and the Effect of Noise", US-Japan Bi-Lateral Seminar in Hydrology, Honolulu, Jan. 1971.

18. Delleur, J. W. and Rao, R. A. "Characteristics and Filtering of Noise in Linear Hydrologic Systems", International Symposium on Mathematical Models in Hydrology", Warsaw, Poland, July 26-31, 1971.

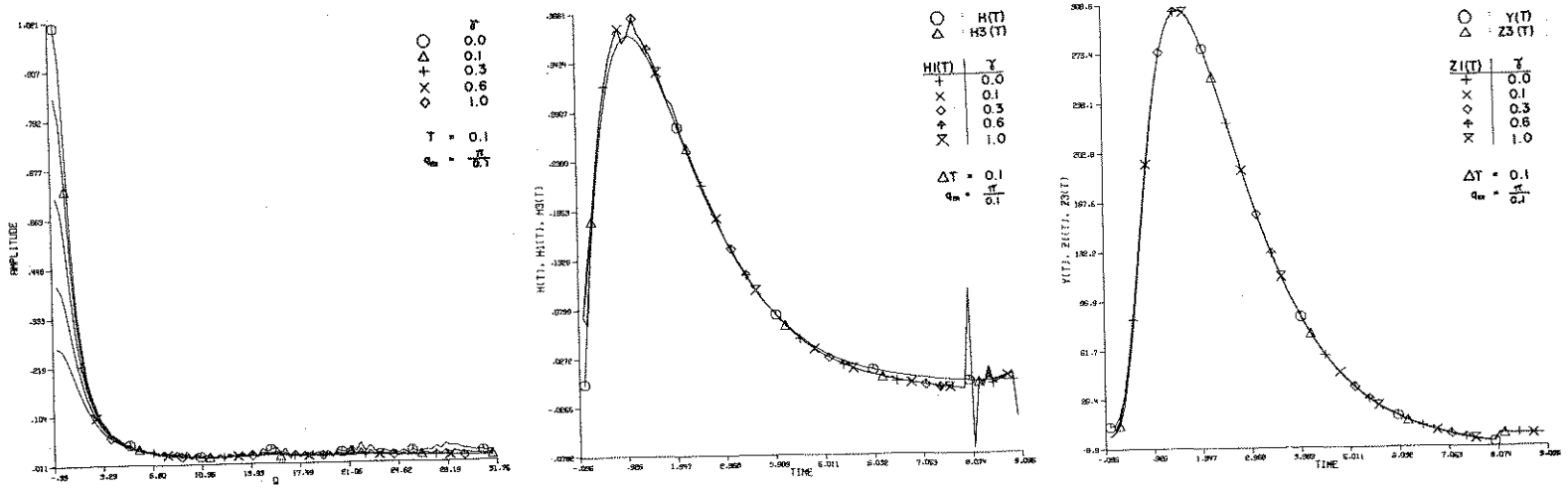

FIG.1 EFFECT OF CHANGE IN γ VALUES IN LAPLACE TRANSFORM - THEORETICAL EXAMPLE

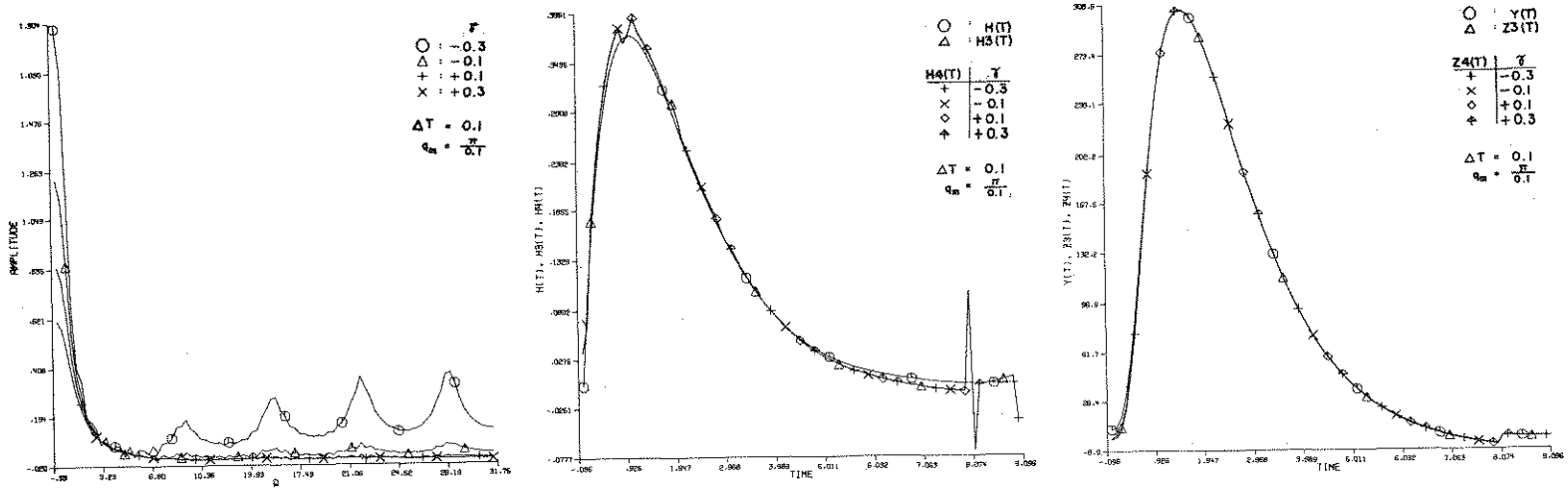

FIG. 2 EFFECT OF NEGATIVE γ VALUES - THEORETICAL EXAMPLE

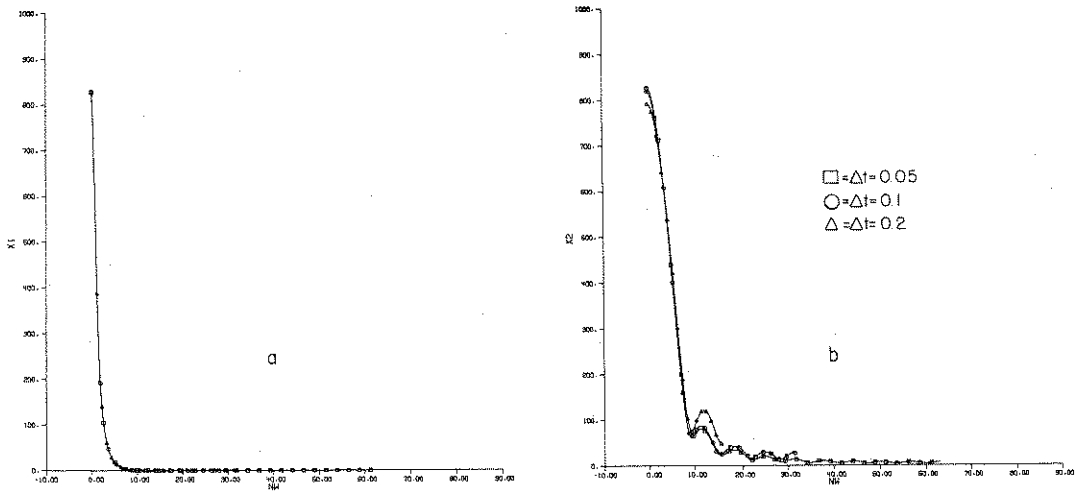

THEORETICAL EXAMPLE

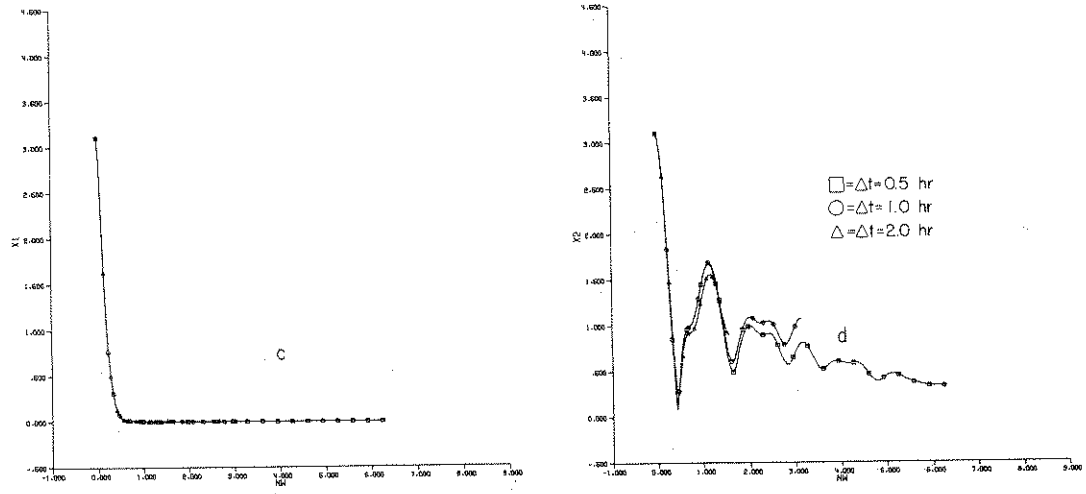

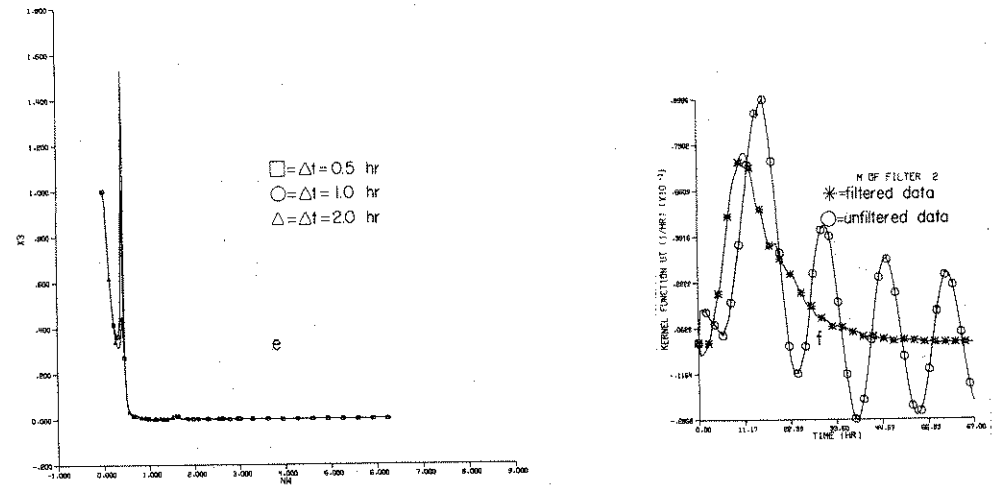

STORM OF 6/22/1960 ON THE
MUSCATATUCK RIVER AT DEPUTY IND

FIG. 3 EFFECT OF DIGITIZATION RATE ON AMPLITUDE SPECTRA AND KERNEL FUNCTION

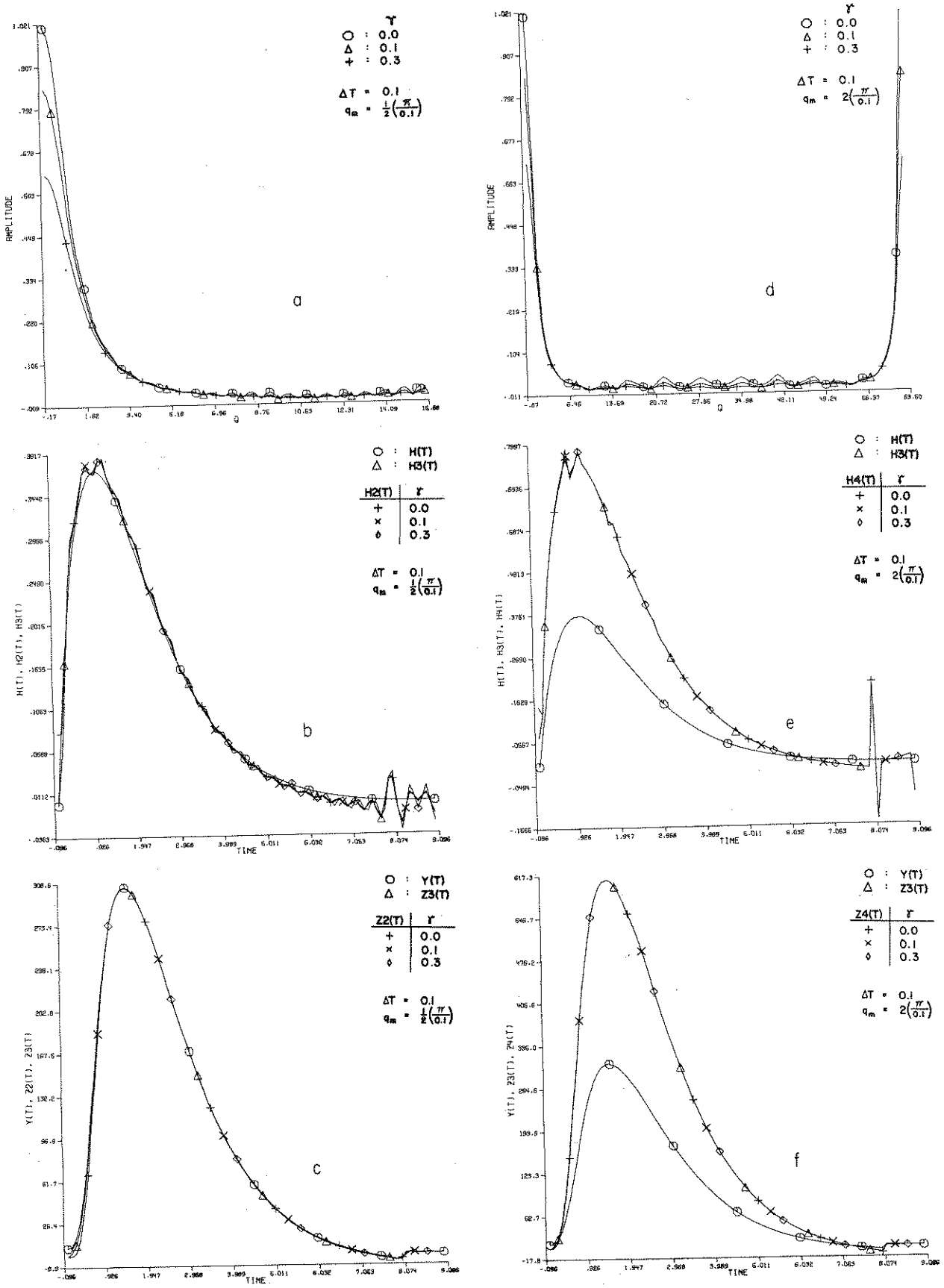

FIG. 4 EFFECT OF VARYING THE TRUNCATION FREQUENCY

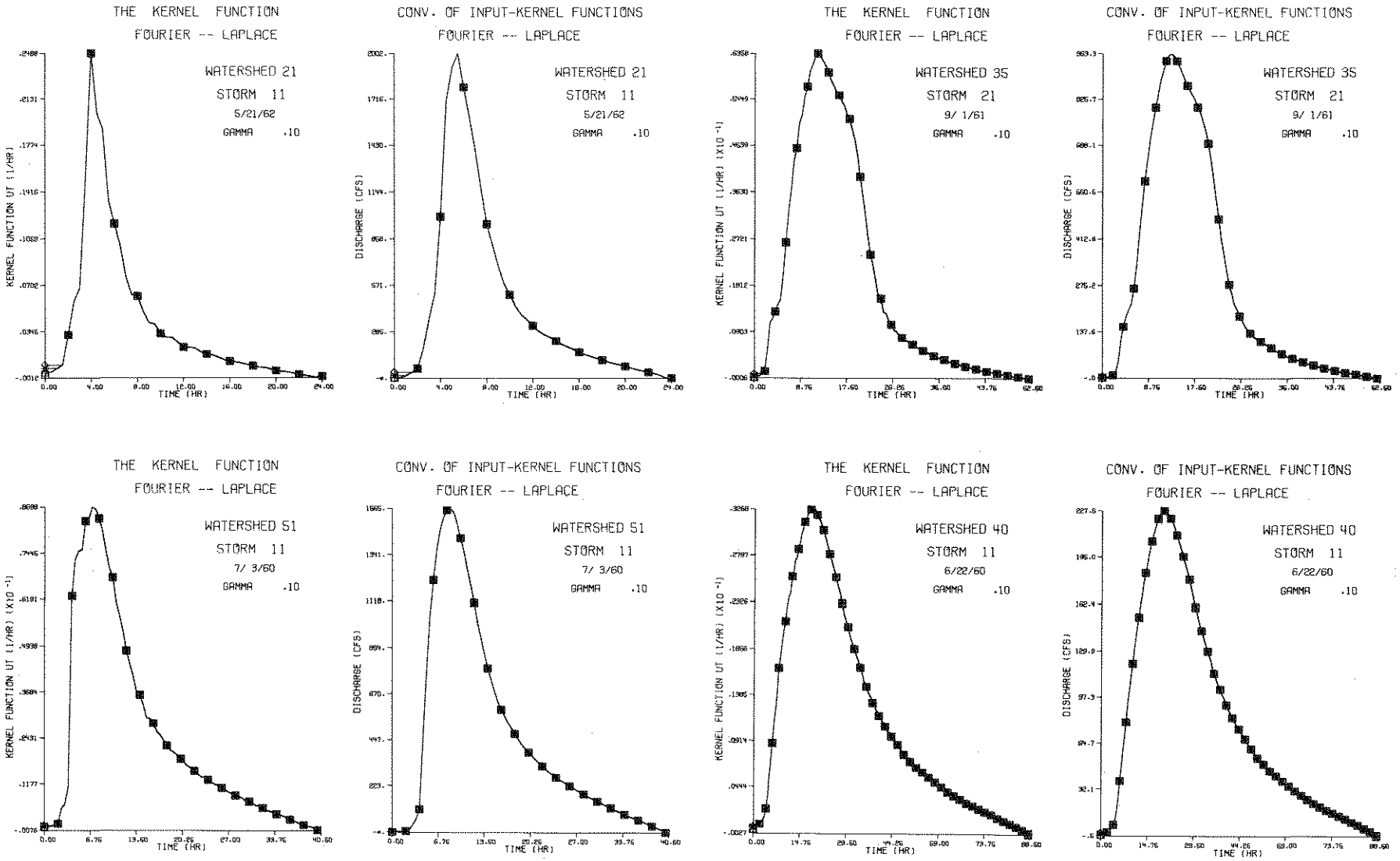

◊ - H1(T), Z1(T); ✳ - H2(T), Z2(T); △ - H3(T), Z3(T); □ - H4(T), Z4(T)

FIG. 5 COMPARISON OF RESULTS BY FOURIER AND LAPLACE TRANSFORMS

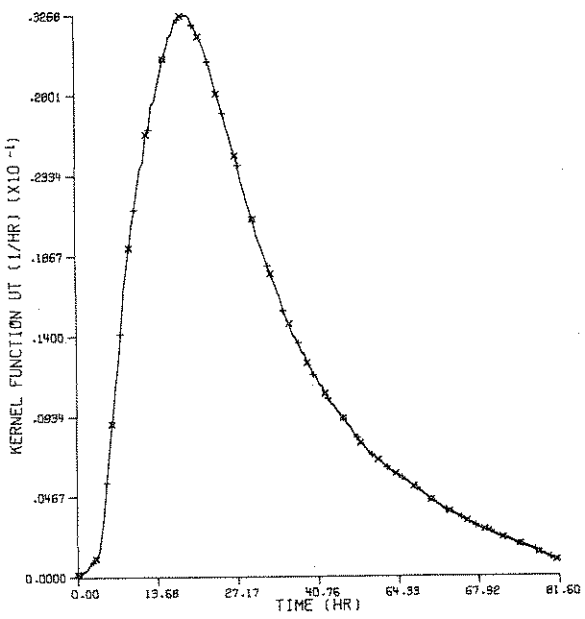

THE KERNEL FUNCTION

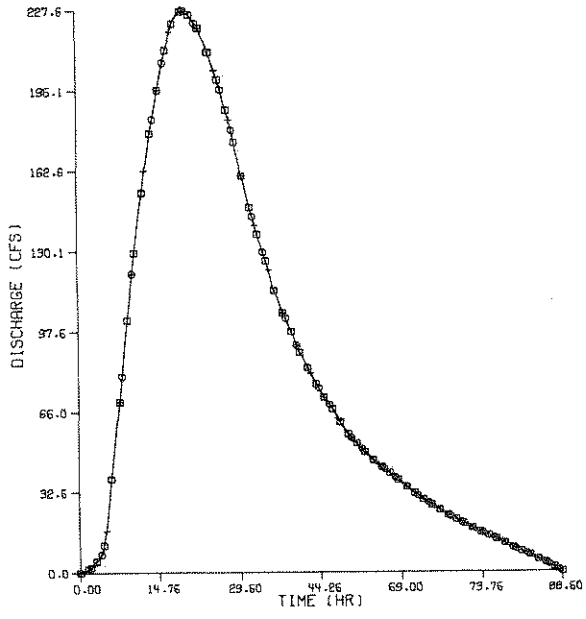

CONV. OF INPUT-KERNEL FUNCTIONS

STORM OF 6/22/60 ON CARPENTER CREEK NEAR EGYPT, INDIANA

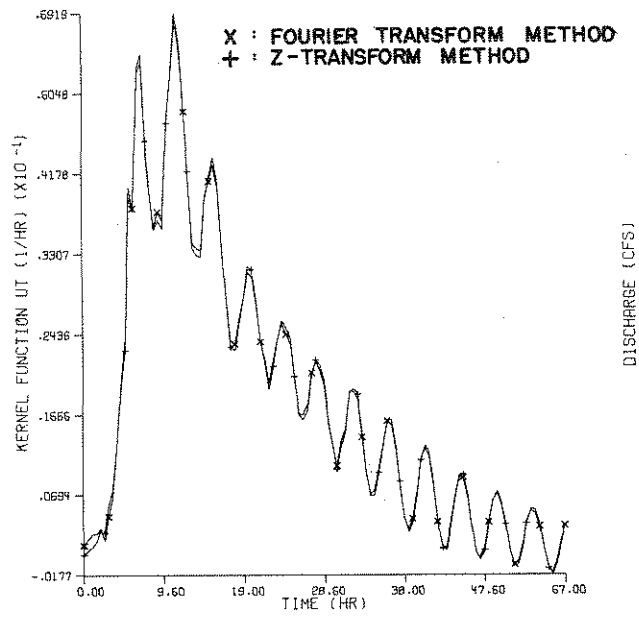

THE KERNEL FUNCTION

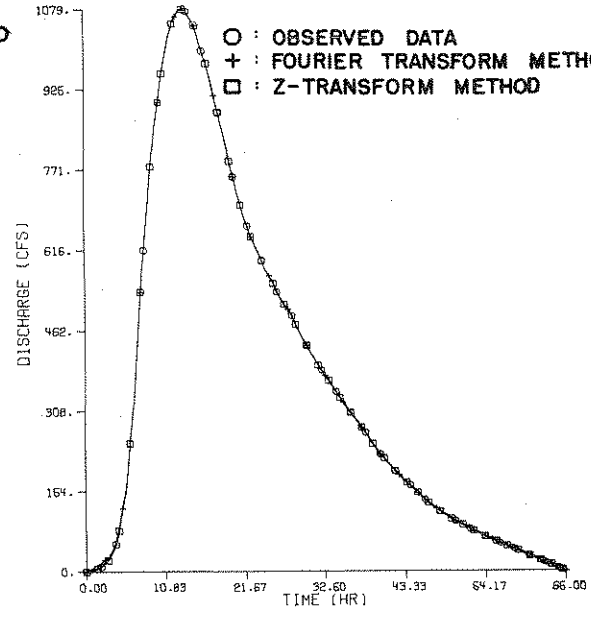

CONV. OF INPUT-KERNEL FUNCTIONS

STORM OF 1/16/53 ON MISSISSINEWA RIVER NEAR RIDGEVILLE, INDIANA

FIG. 6. Z-TRANSFORM METHOD

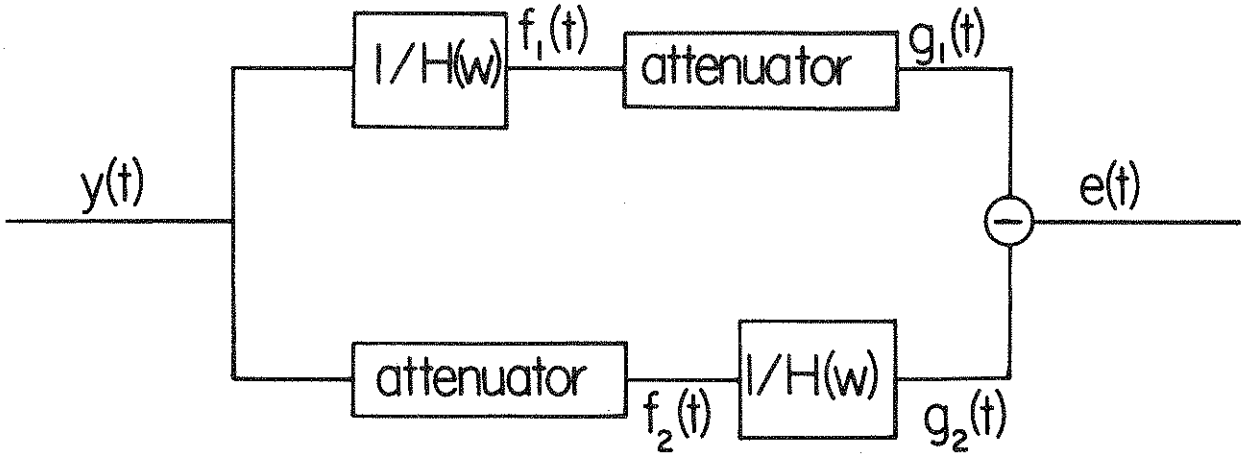

FIG. 7.

COMPUTATIONAL SCHEME FOR NOISE EVALUATION.

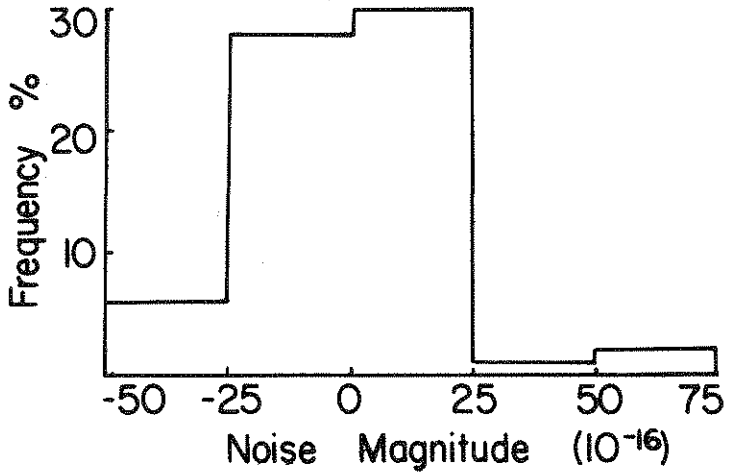

FIG. 8.

NOISE PROBABILITY DISTRIBUTION FOR 3 STORMS.

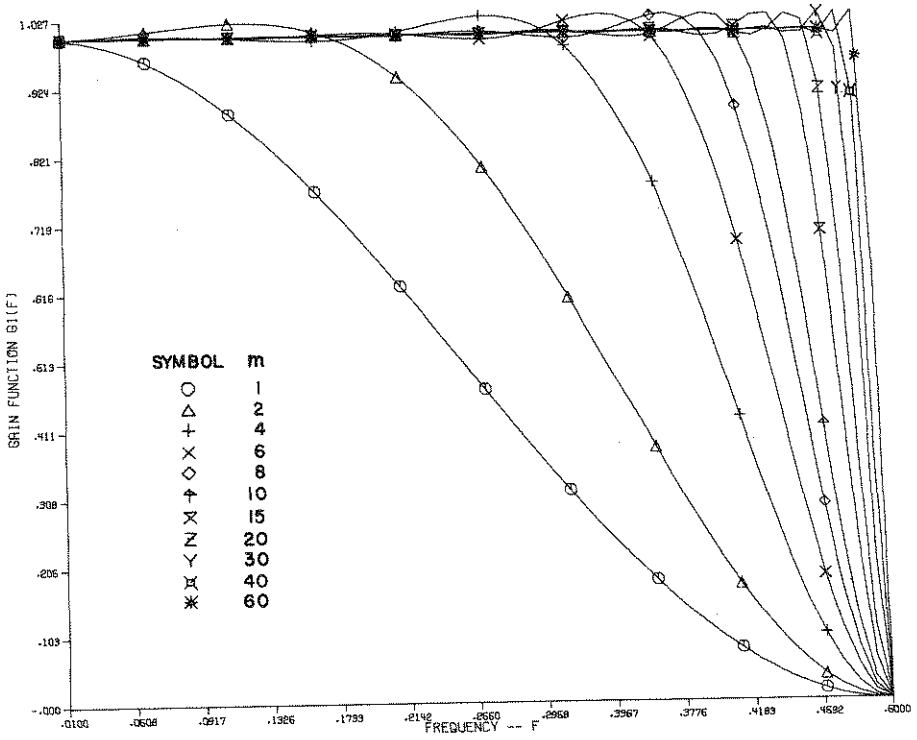

MODIFIED JENKINS FILTER

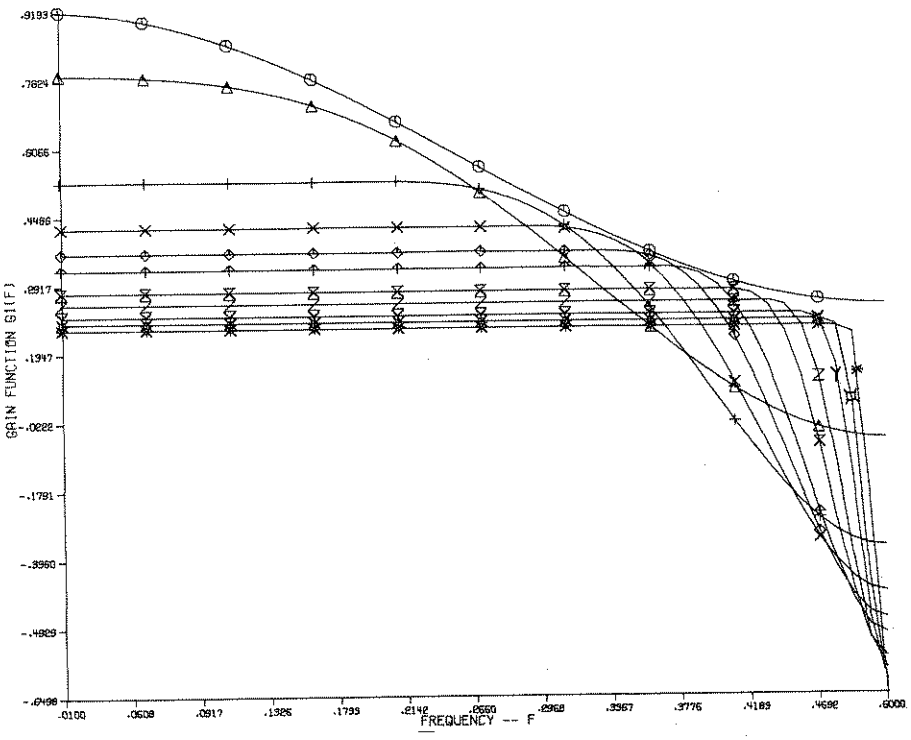

MODIFIED BLACKMAN FILTER

FIG. 9. LOW PASS FILTER FREQUENCY RESPONSE

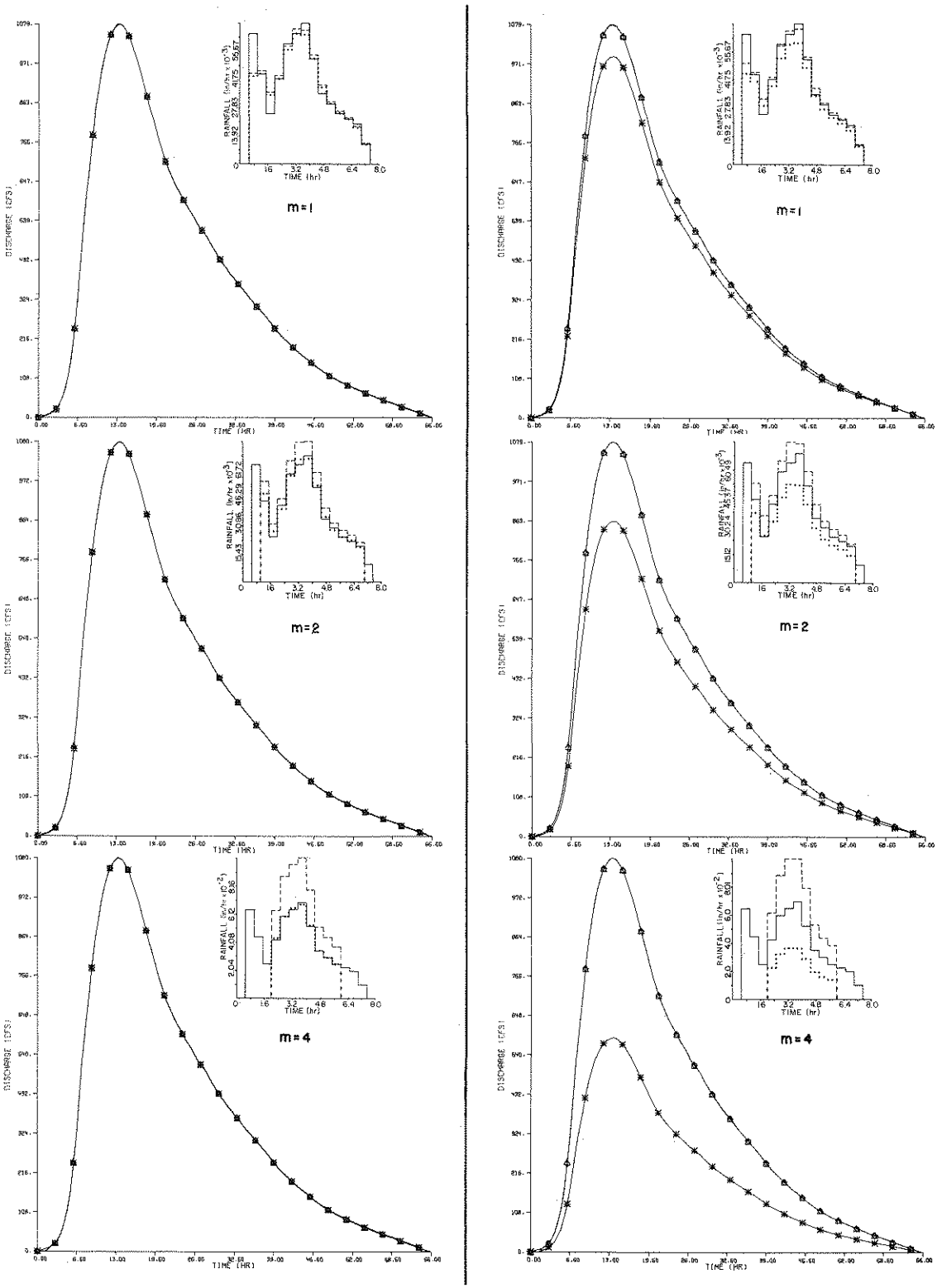

RAINFALL: — ORIGINAL DATA, ···· FILTERED DATA, --- ADJUSTED DATA. RUNOFF: △ ORIGINAL DATA, ✳ FILTERED DATA, ◇ ADJUSTED DATA.

STORM OF 1/16/53 ON MISSISSINEWA RIVER NEAR RIDGEVILLE, INDIANA

FIG.10 EFFECT OF FILTERING ON THE ORIGINAL DATA

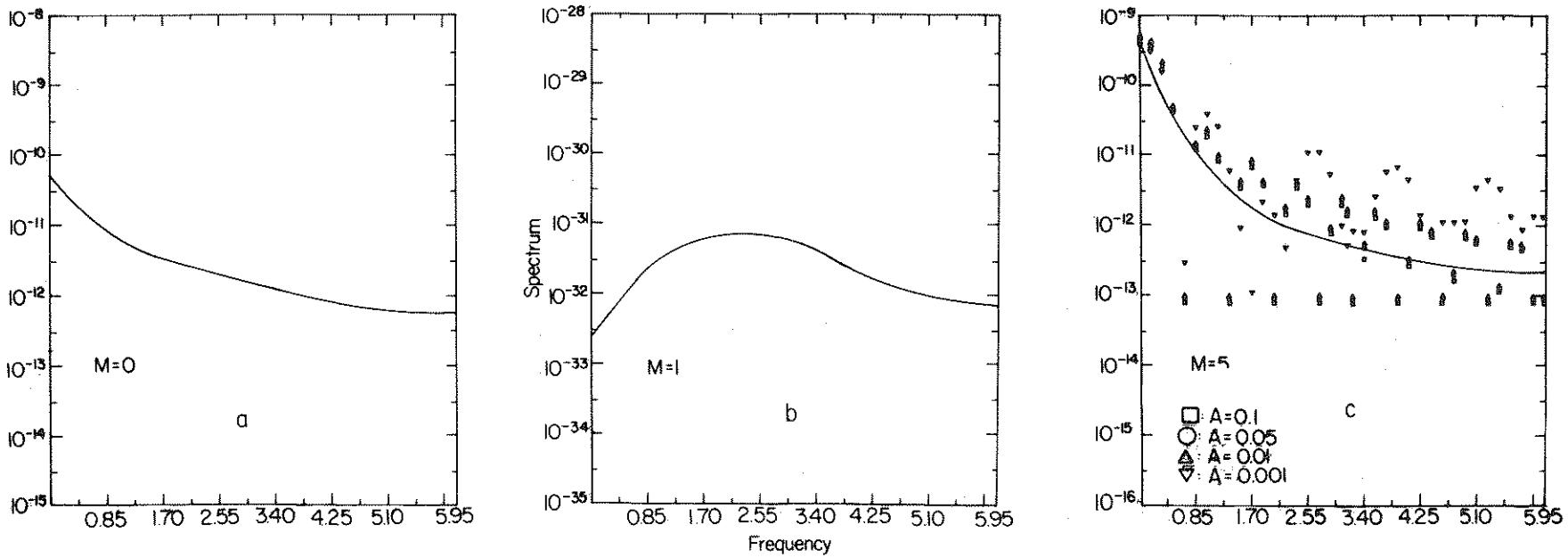

FIG.11. EFFECT OF FILTERING ON NOISE SPECTRUM

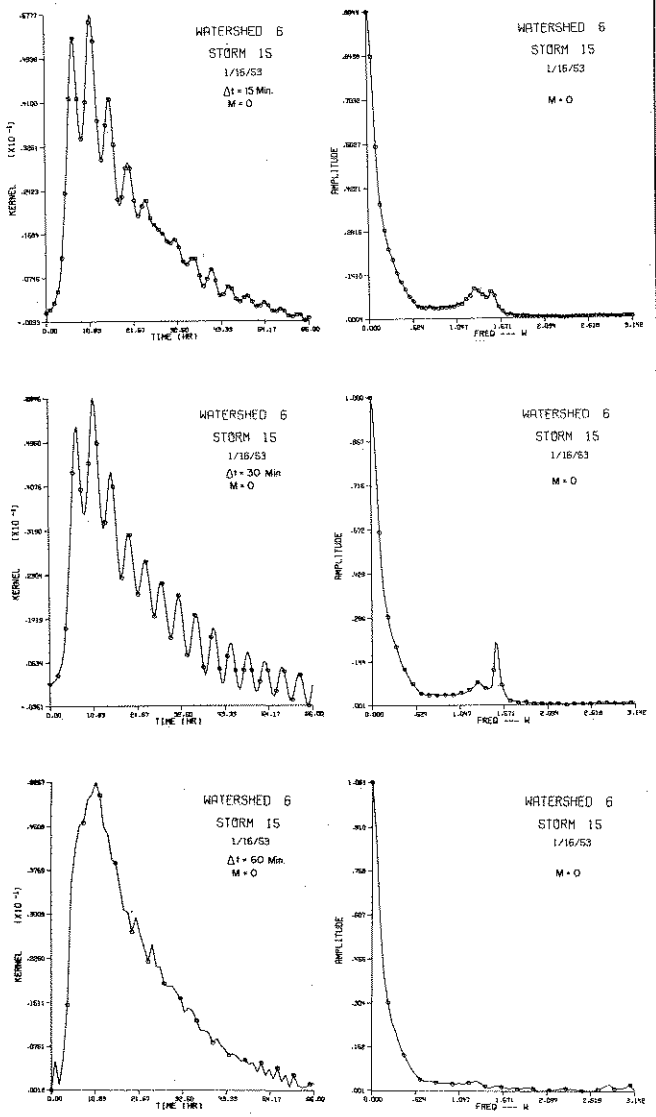

FIG. 12a EFFECT OF ORDINATE SPACING

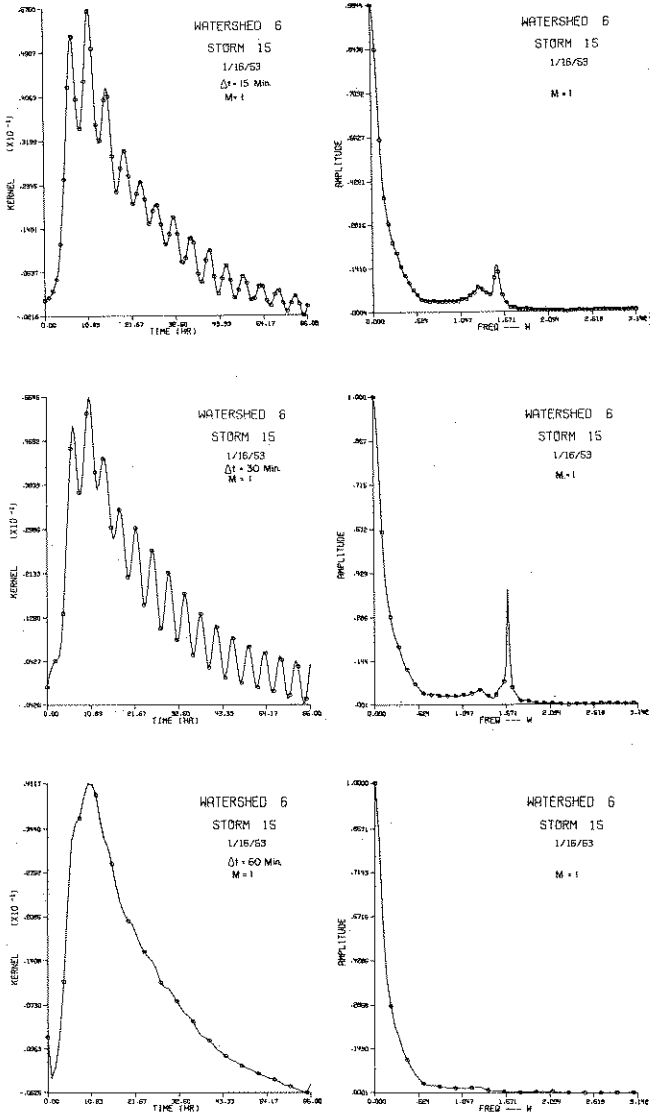

FIG. 12b COMBINED EFFECT OF ORDINATE SPACING AND FILTERING

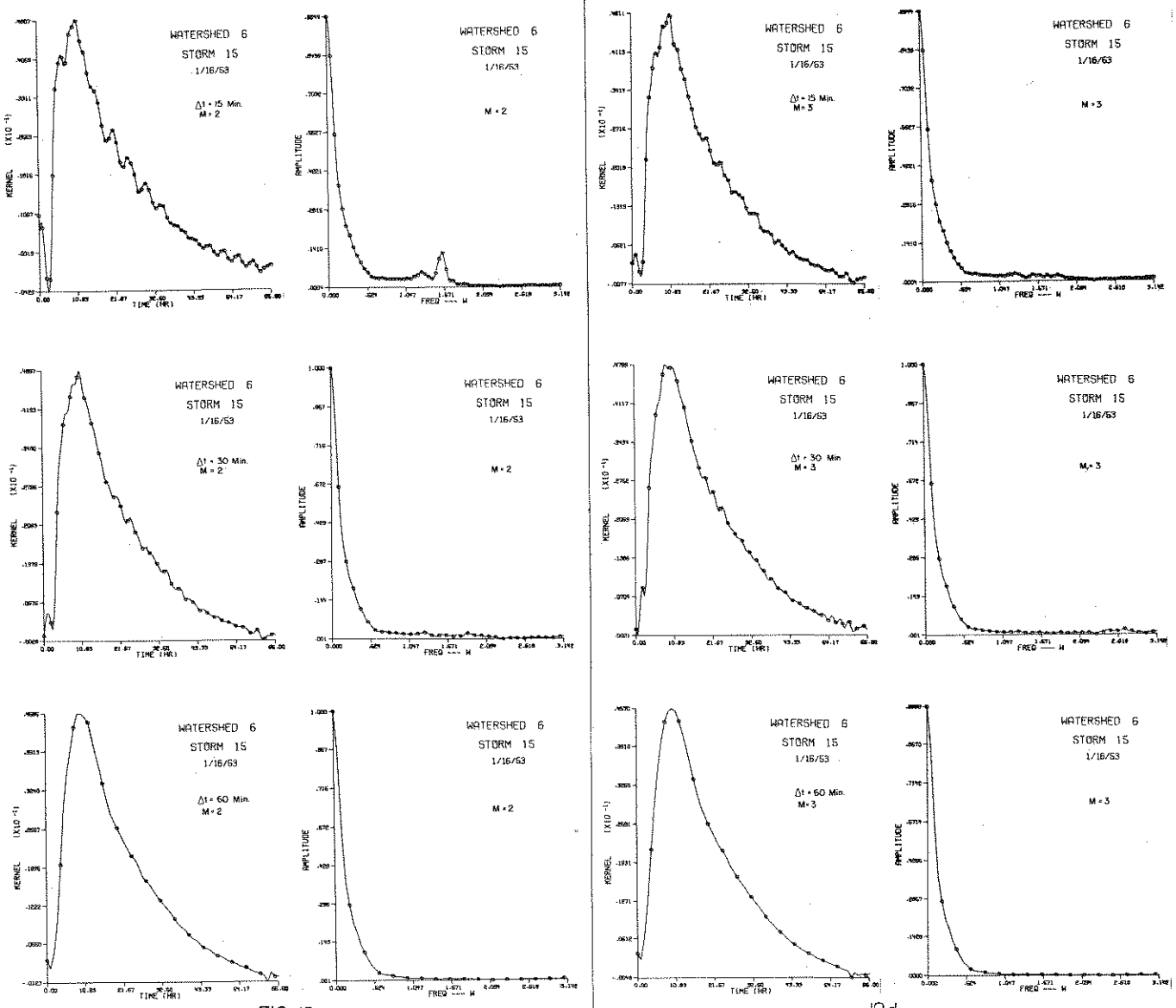

FIG. 12c

12d

COMBINED EFFECT OF ORDINATE SPACING AND FILTERING (CONTINUED)

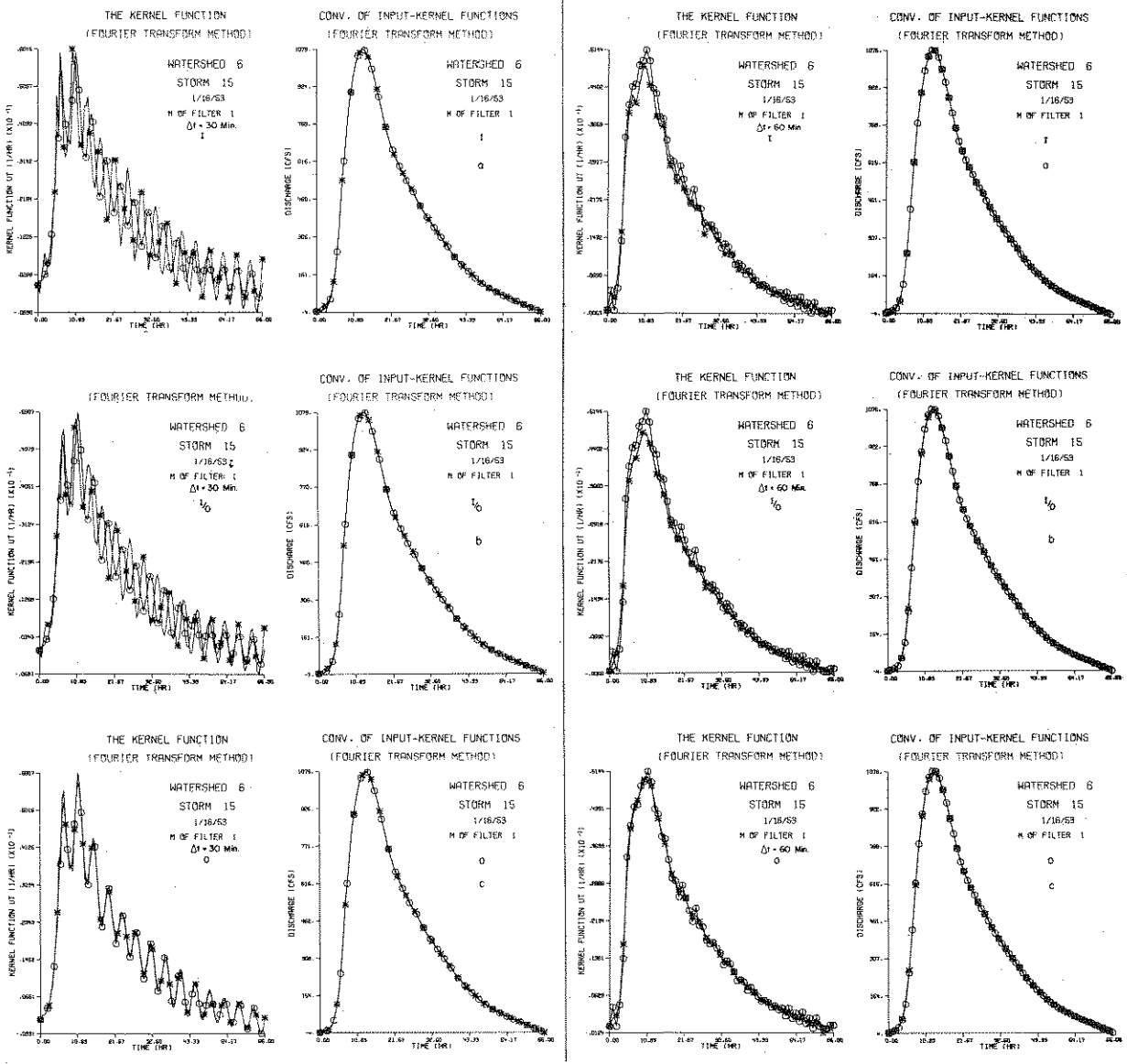

I - INPUT FILTERED, O - OUTPUT FILTERED, I/O - INPUT & OUTPUT FILTERED. MODIFIED JENKINS FILTER

FIG.13 FILTERING INPUT, OUTPUT OR BOTH

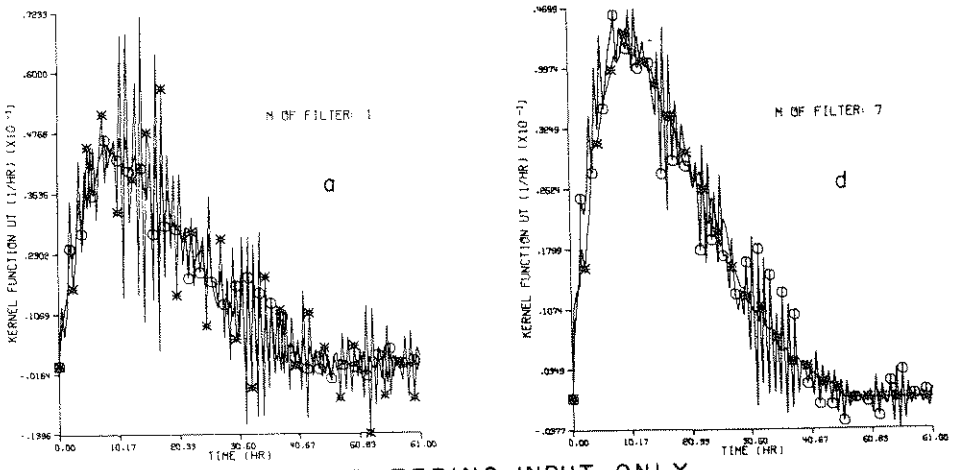

FILTERING INPUT ONLY

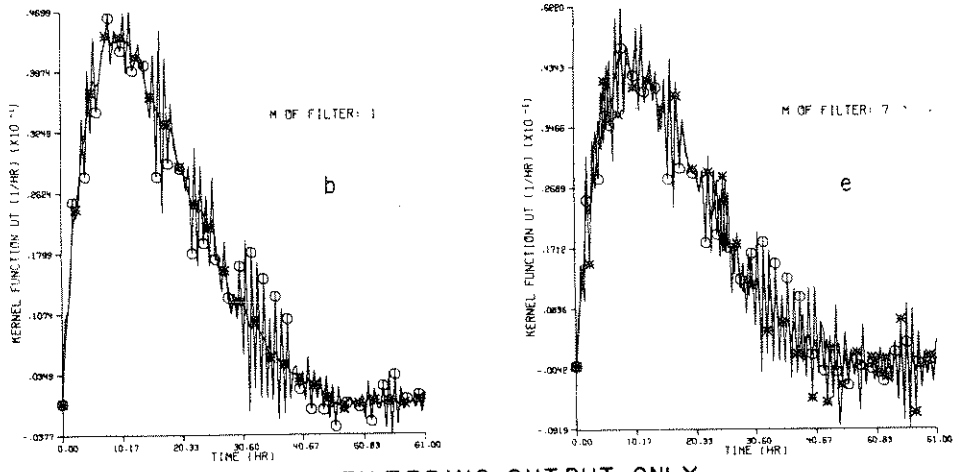

FILTERING OUTPUT ONLY

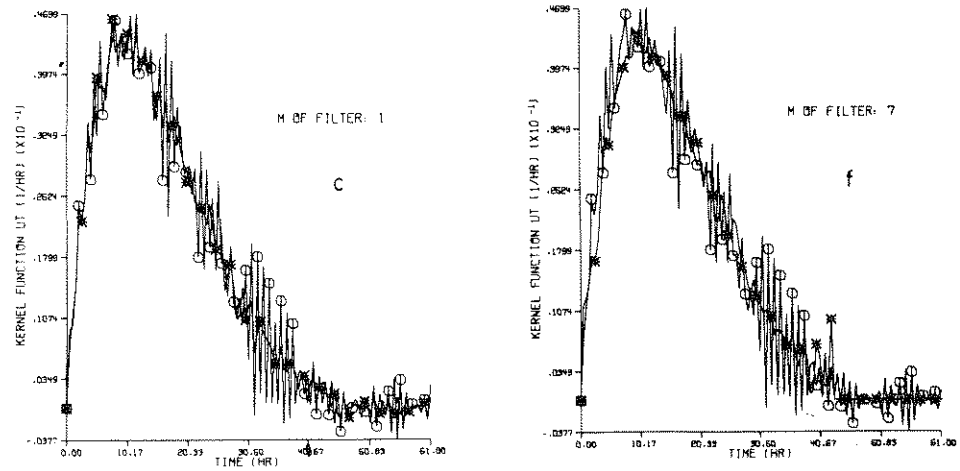

FILTERING INPUT AND OUTPUT

○ ORIGINAL DATA, ✳ FILTERED AND ADJUSTED DATA, ΔT=0.5 HR.

STORM OF 2/17/56 ON MISSISSINEWA RIVER NEAR RIDGEVILLE, INDIANA

FIG. 14 EFFECT OF INCREACING THE FILTER ORDER

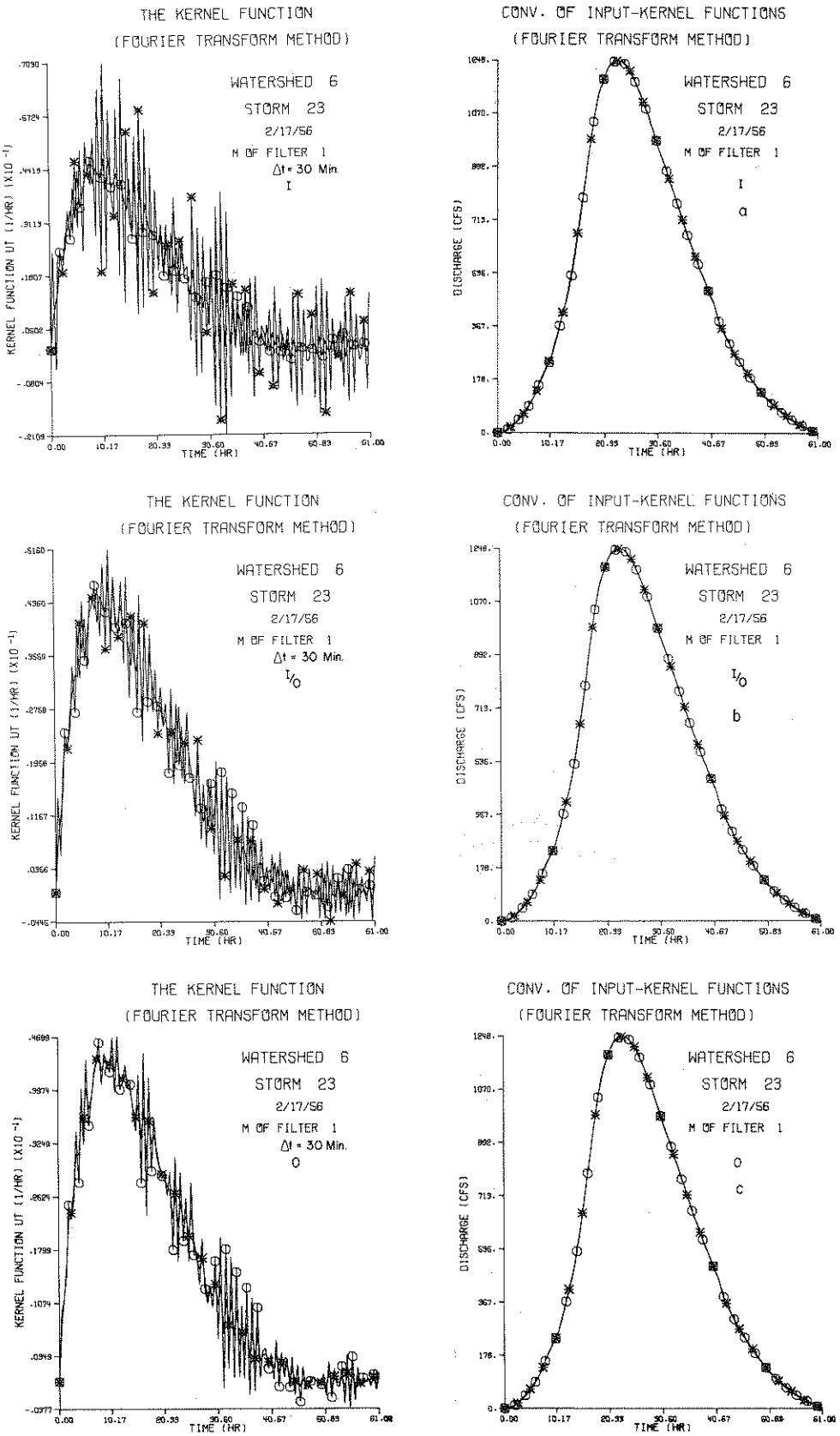

I - INPUT FILTERED, O - OUTPUT FILTERED, I/O - INPUT & OUTPUT FILTERED. MODIFIED BLACKMAN FILTER

FIG. 15 RESULTS WITH THE MODIFIED BLACKMAN FILTER

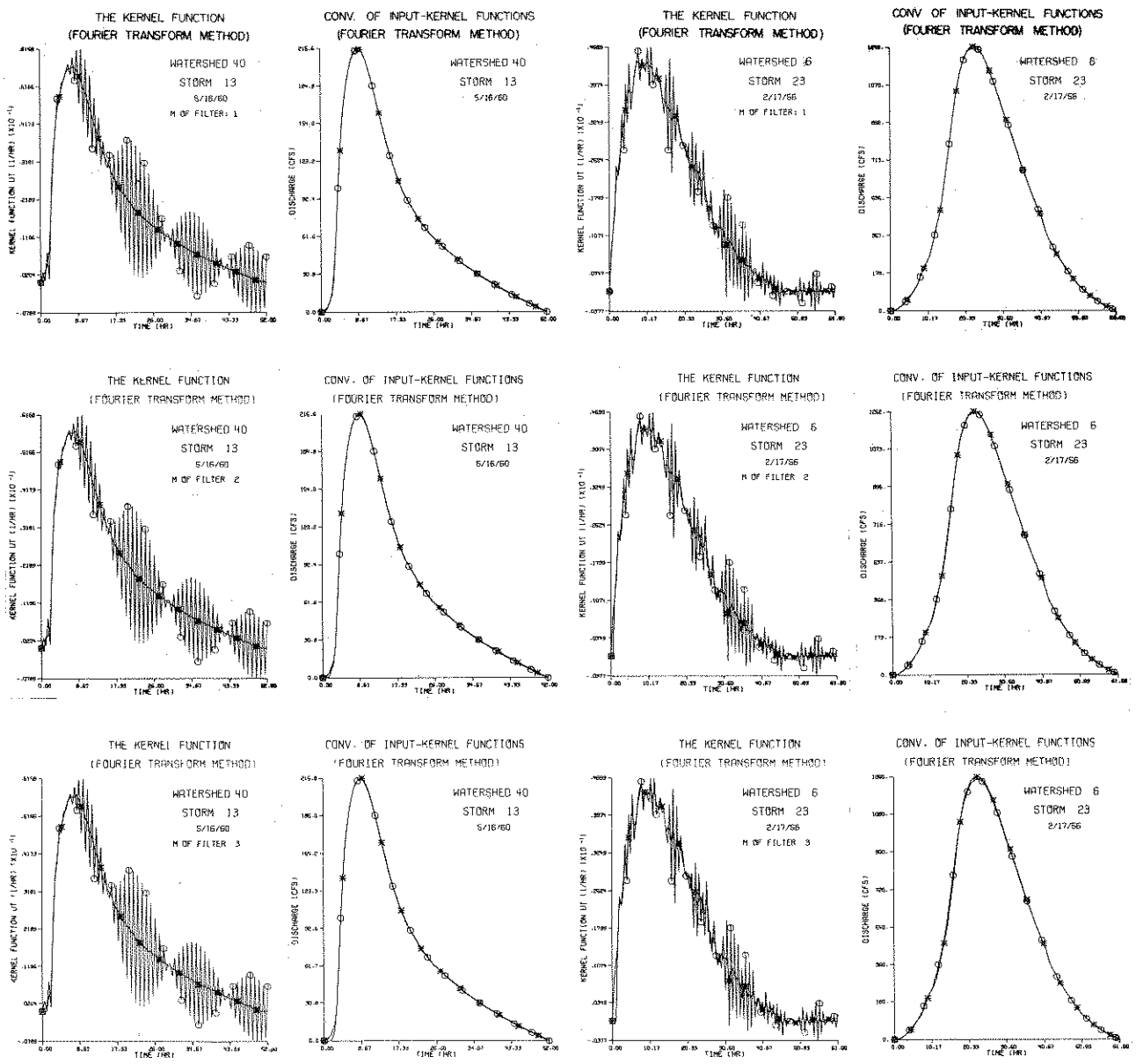

FIG.16 FILTERING THE KERNEL FUNCTION IN THE TIME DOMAIN

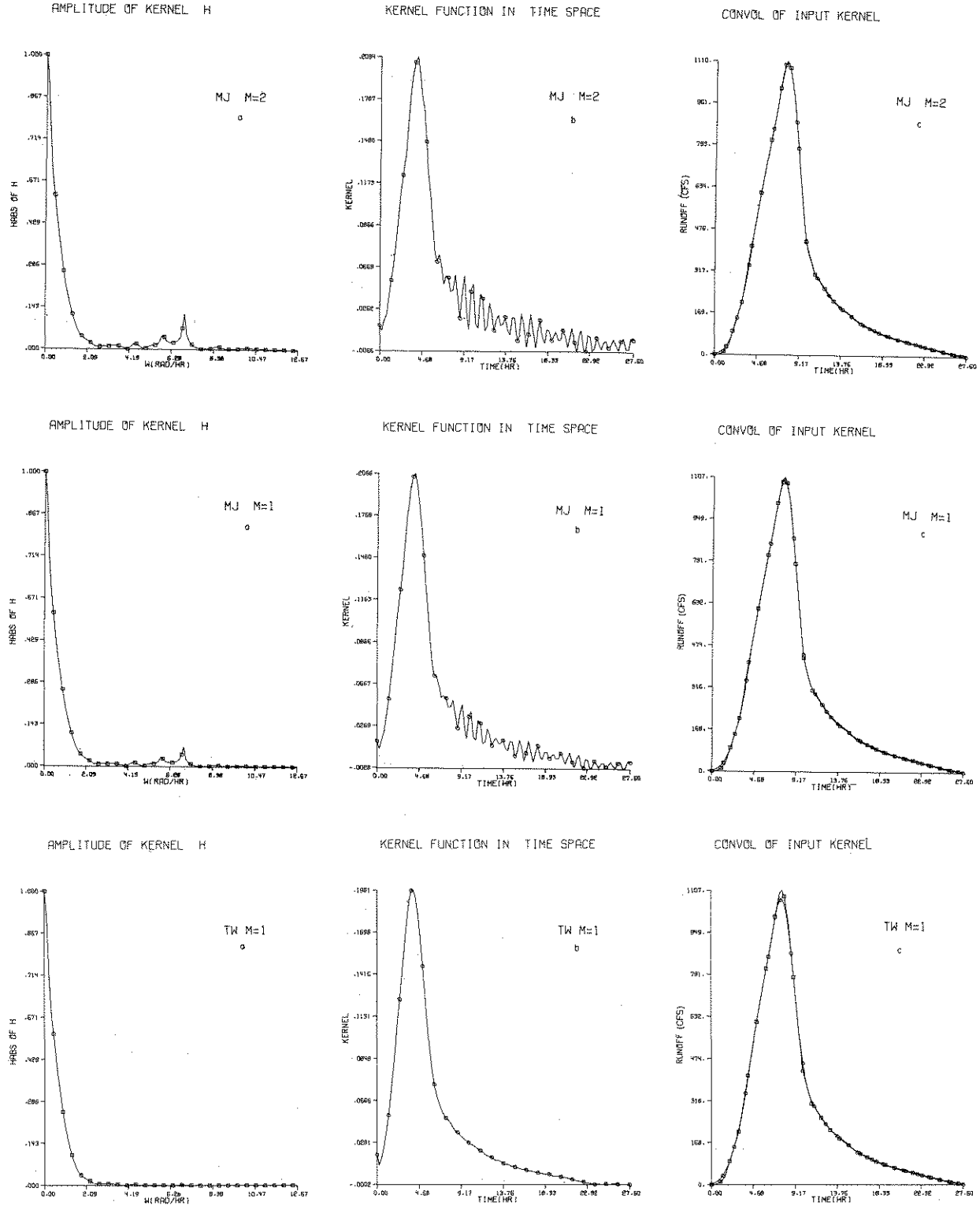

a - AMPLITUDES, b - KERNEL FUNCTION IN TIME SPACE, c - CONVOLUTION OF INPUT-KERNEL FUNCTION
MJ - MODIFIED JENKINS WINDOW, TW - TUKEY WINDOW
STORM OF 4/25/61 ON BEAN BLOSSOM CREEK NEAR BEAN BLOSSOM, INDIANA

FIG.17 SMOOTHING THE FREQUENCY RESPONSE IN THE FREQUENCY DOMAIN

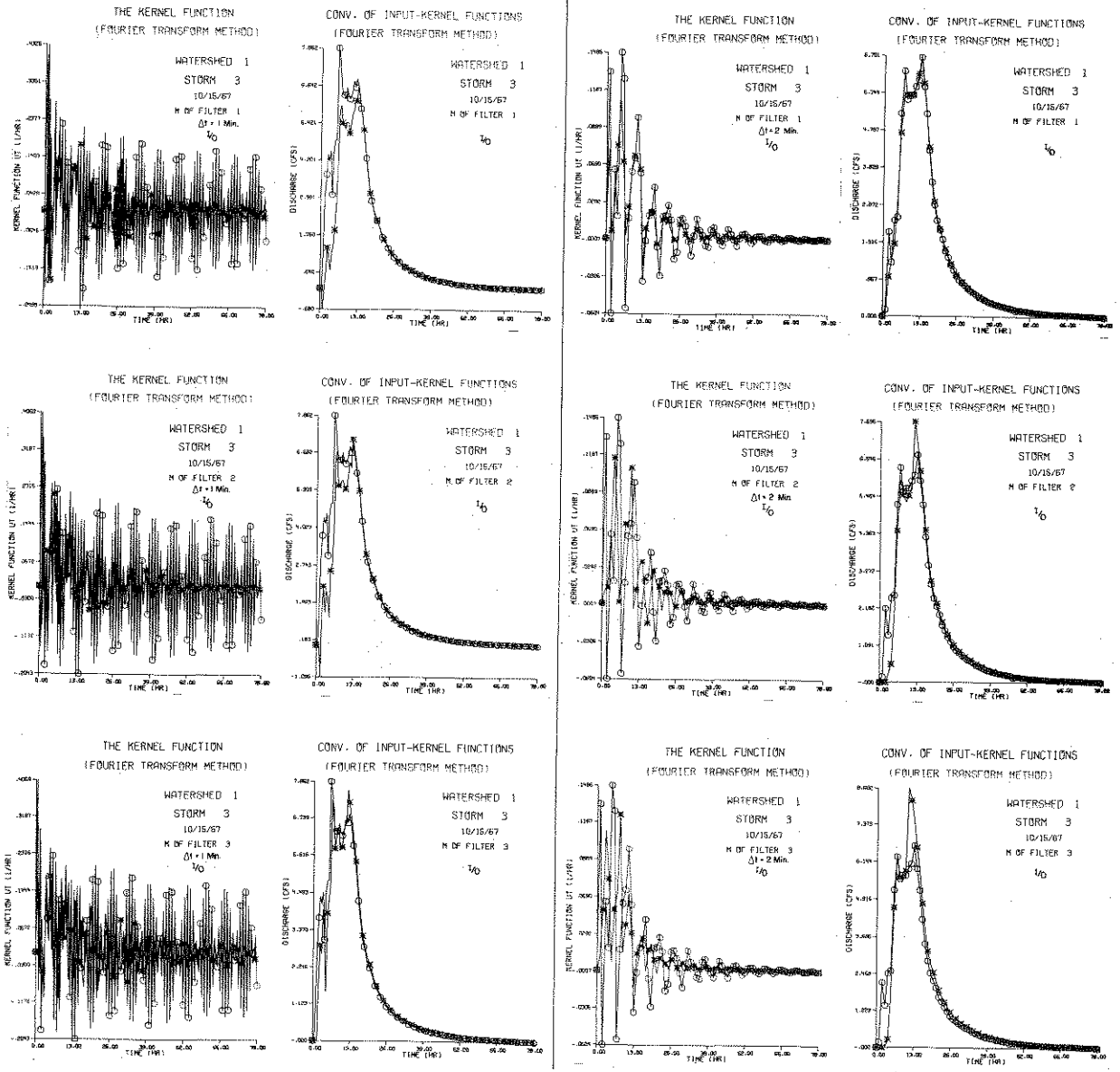

I/O - INPUT AND OUTPUT FILTERED; O - OBSERVED VALUES; # FILTERED AND REGENERATED VALUES. MODIFIED JENKINS FILTER

FIG 18a EFFECT OF CHANGE IN DISCRETIZATION RATE AND OF FILTERING ON DATA FROM A SMALL URBAN WATERSHED

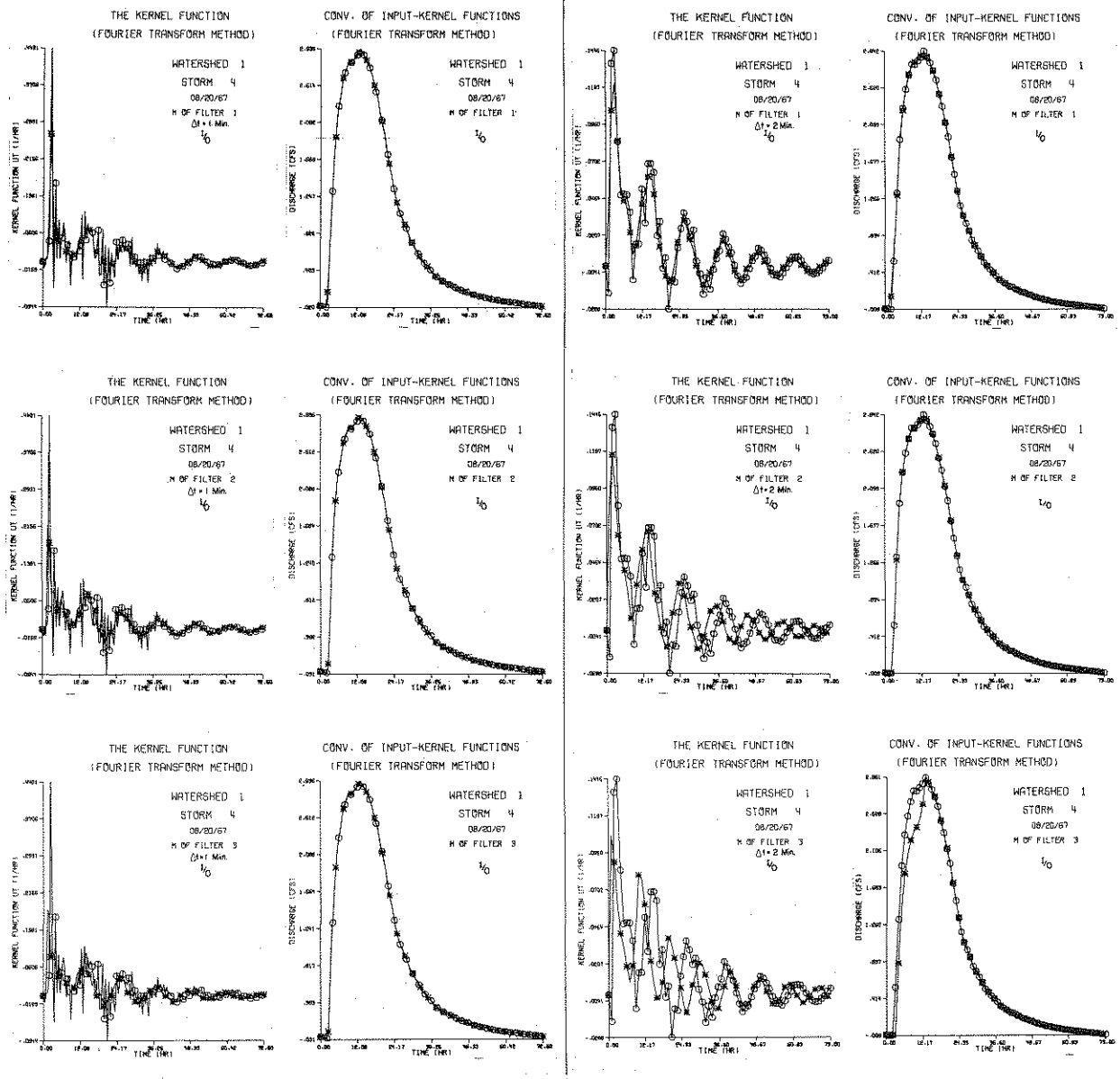

FIG. 18b EFFECT OF CHANGE IN DISCRETIZATION RATE AND OF FILTERING ON DATA FROM A SMALL URBAN WATERSHED (CONTINUED)